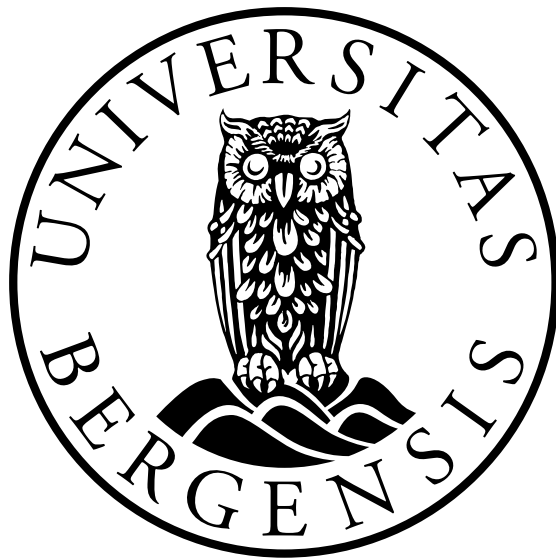


Geological Storage of CO₂: Sensitivity and Risk Analysis

Meisam Ashraf



Dissertation for the degree of Philosophiae Doctor (PhD)

Department of Mathematics
University of Bergen

November 2012

Scientific environment

This dissertation is submitted as a partial fulfillment of the requirements for the degree Doctor of Philosophy (PhD) at the University of Bergen. It is part of the project Mathematical Modeling and Risk Assessment of CO₂ storage, MatMoRA, which is funded by the Norwegian Research Council, Statoil and Norske Shell under grant no. 178013/I30 and lead by Professor Helge Dahle at the Department of Mathematics, University of Bergen (UiB).

The working environment have been SINTEF-ICT in Oslo, and CIPR in Bergen, and SIMTECH in Stuttgart. The chief scientist at SINTEF-ICT, professor Knut-Andreas Lie, has been the main adviser and Professor Jan M. Nordbotten at the Department of Mathematics, UiB, along with the research scientist at SINTEF, Halvor M. Nilsen, have been the co-advisers. With warm supports from professor Rainer Helmig, head of department of hydromechanics and modelling of hydrosystems at Stuttgart university, last parts of the work is benefited from advices of professor Wolfgang Nowak, head of Stochastic modelling of hydrosystems, Dr. Sergey Oladyshkin, postdoctoral fellow at SIMTECH, and professor Holger Class at Stuttgart university.

Acknowledgements

I dedicate this to my father, who wished to do a PhD, but the situation did not help him.

I would like to appreciate my decision to do a PhD after years of being in the industry . My first motivation was to experience the educations in a mathematical environment. I was very pleased and lucky to work with the best mathematicians in Norway on the topic of CO₂ storage.

First and foremost, Knut-Andreas Lie was more than an adviser for me, whom I had the chance and honor to work with closely and in a daily-based manner. I learned a lot from discussions with Halvor M. Nilsen, initially my only friend in Norway, when I left my family and friends and moved to start the program. Jan M. Nordbotten always inspired me and made me to love mathematics even more. Helge Dahle warmly helped me with every aspect of my studies. Maria Elenius gave me the enthusiasm as a colleague to enjoy my research. I enjoyed being an office-mate at SINTEF with Christian Schulz. Arne Skorstad is among those whom I was proud to work with. I was lucky to work with Princeton people, Michael Celia and Sarah Gasda. I enjoyed learning from Ivar Aavatsmark, Hans Munthe-Kaas, and Anette Stephansen. And many friends in Bergen Math. department that I always enjoyed discussing interesting topics with them.

During this program I had the chance to spend one semester in Stuttgart to work with mathematicians on stochastic analysis. I was proud to be sitting in the group of Rainer Helmig, to enjoy time with such a live and friendly research group. Thanks to Stuttgart people, one by one, for such a nice social time that I had over there. I had very constructive scientific discussions with Segrey Oladyshkin and Wolfgang Nowak, Holger Class, and Anozie Ebigboe. I extremely enjoyed working with them.

I would like to thank my manager at my new employer, Ed Leung, for supporting me to finish my thesis.

And thanks to the coffee machine and printer at SINTEF-ICT, for helping me a lot in writing this report.

Abstract

In the context of geological CO₂ storage, one main uncertainty that makes the prediction of operational success more complicated, is the geological heterogeneity in the system. The CO₂ storage capacity and risk of leakage from the storage location are highly sensitive to the geological modeling of the problem. The main motivation of our works is to address the importance of proper geological modeling and to provide a practical work-flow for assessing the geological uncertainty consequences in the operations.

We choose the shallow-marine depositional system for our studies, but the same method could be implemented for any other types. The study is based on large number of geological realizations with different levels of heterogeneity. The heterogeneity is modeled by the main geological parameters and used to discuss the flow responses that are important in the storage of CO₂. Among those parameters are the aggradational angle, levels of barriers in the system, faults, lobosity, and progradation direction.

We describe the flow behavior in terms of flow responses that can be used to evaluate the performance of geological storage of CO₂ in the aquifers and abandoned oilfields. The injected plumes of CO₂ are analyzed for their volumes and numbers and their dynamics in the system. Detailed sensitivity analysis and risk assessment are performed on the designed injection and early migration study. The geological parameters are ranked based on their influence on the flow response variations. No general conclusion for uncertainty assessment is expected from our studies, since this may change in different geological regions. However, we demonstrate a practical work-flow that can be used in any uncertainty assessment project.

We mainly consider the injection and early migration of CO₂ as this work is part of a project that covers the long-term CO₂ migrations. Nevertheless, the discussions and results here can be used with some modifications (such as extending the model spatial extent) in the long-term migrations.

The work is presented and published in many scientific conferences in the form of proceedings, posters, and seminars. Some parts are submitted to the literature and are in their way to be published in the literature.

List of papers

1. M. Ashraf, K.A. Lie, H.M. Nilsen, J.M. Nordbotten & A. Skorstad, *Impact of geological heterogeneity on early-stage CO₂ plume migration*, XVIII International Conference on Water Resources (CMWR 2010), J. Carrera (Ed), CIMNE, Barcelona, 2010.
2. M. Ashraf, K.A. Lie, H.M. Nilsen & A. Skorstad, *Impact of geological heterogeneity on early-stage CO₂ plume migration: sensitivity study*, Proceedings of the 12th European Conference on the Mathematics of Oil Recovery (ECMOR XII), Oxford, UK, 6-9 September 2010.
<http://www.earthdoc.org/publication/publicationdetails/?publication=41331>
3. M. Ashraf, K.A. Lie, H.M. Nilsen & A. Skorstad, *Impact of geological heterogeneity on early-stage co₂ plume migration: CO₂ distribution sensitivity study*, submitted to the International Journal of Greenhouse Gas Control(IJGGC).
4. M. Ashraf, *Impact of geological heterogeneity on early-stage co₂ plume migration: pressure sensitivity study*, submitted to the International Journal of Greenhouse Gas Control(IJGGC).
5. M. Ashraf, S. Oladyshkin, W. Novak, *Geological storage of CO₂: global sensitivity analysis and risk assessment using the arbitrary polynomial chaos expansion*, Proceedings of the European Geosciences Union (EGU) General Assembly 2012, April, Vienna, Austria, Geophysical Research Abstracts., Vol. 14, EGU2012-9243. Submitted to special issue of the International Journal of Greenhouse Gas Control(IJGGC), in second review.

Contents

Scientific environment	i
Acknowledgements	iii
Abstract	v
List of papers	vii
1 Introduction	1
1.1 Introduction	2
1.2 Carbon storage	3
1.3 Modeling procedure	4
1.4 Uncertainty Sources	6
1.5 Geological modeling	7
1.5.1 Geological description	7
1.5.2 Geological parameters	10
1.6 Flow equations	16
1.6.1 Single phase flow	16
1.6.2 Two-phase flow	18
1.7 Flow regimes	22
1.7.1 Injection and early migration	23
1.7.2 Long term migration	25
1.8 Vertical averaging	26
1.9 Flow modeling	28
1.9.1 Numerical scheme	28
1.9.2 Flow scenarios	30
1.9.3 Flow responses	32
1.10 Sensitivity and risk analysis	36
1.10.1 Stochastic analysis	36
1.10.2 Arbitrary polynomial chaos expansion	37
1.10.3 Sensitivity analysis	39
1.10.4 Risk analysis	42
1.11 Implementation of work-flow	42
2 Introduction to the papers	45
2.1 Introduction	46
2.2 Summary of papers	46

3 Scientific results	51
3.1 Impact of geological heterogeneity on early-stage CO ₂ plume migration: pressure behavior study	53
3.2 Geological storage of CO ₂ : heterogeneity impact on pressure behavior .	57
3.3 Geological storage of CO ₂ : global sensitivity analysis and risk assessment using the arbitrary polynomial chaos expansion	61

List of Figures

1.1	Green-house gases act like a blanket trapping the heat received from the sun.	3
1.2	Geological sequestration is a proposed solution for mitigating the industrial CO ₂ emissions.	4
1.3	Modeling procedure diagram.	5
1.4	bla bla bla	11
1.5	bla bla bla	12
1.6	bla bla bla	12
1.7	bla bla bla	13
1.8	bla bla bla	14
1.9	Lobosity levels are defined based on the shoreline shape, which is caused by the interplay between fluvial and wave forces.	15
1.10	Barrier levels caused by periodic floods.	15
1.11	Aggradation angle levels.	16
1.12	Progradation levels.	16
1.13	Flow domain and boundaries.	17
1.14	Permeability is an idication of how easy it is for the fluids to flow trough the medium.	17
1.15	Wettability and interfacial tension in water-CO ₂ system.	18
1.16	Multi-phase flow in the pore scale.	19
1.17	Two-phase flow and relative permeability.	19
1.18	Capillary pressure can be expressed as a function of wetting saturation. The plot is a typical curve of capillary pressure function with a maximum of $P_{c\max}$	20
1.19	Capillary pressure distribution in the transition zone.	21
1.20	Saturation distribution in the capillary transition zone.	21
1.21	Flow regimes in geological CO ₂ storage.	26
1.22	Hydrostatic equilibrium condition results in three zones: the CO ₂ zone with thickness h_{co_2} , the water table with thickness h_w , and the capillary transition zone h_{pc}	28
1.23	Transmissibility calculation for two cells a and b.	29
1.24	Well modeling inside a simulation cell.	30
1.25	Top, bottom, and upper side boundaries are closed and the rest are open to the flow.	31
1.26	External pressure drive.	32
1.27	Mobile and residual CO ₂ volume.	32

1.28 We use a 2D Gaussian distribution for leakage probability on the cap-rock.	33
1.29 Marker codes used to plot the simulation results of all cases together.	34
1.30 Marker codes used to plot the simulation results of all cases together.	34
1.31 Collocation points are combined in different uncertainty directions such that the total probability in all directions is maximized.	39
1.32 Flow-chart of work process implemented in an automated procedure.	42

Chapter 1

Introduction

1.1 Introduction

“We won’t have a society if we destroy the environment”

– Margaret Mead, American cultural anthropologist, 1901-1978

The commencement of industrial revolutions in the last centuries is closely related to the outbreak of environmental damages and harmful manipulation of ecosystems. Environmental issues are actual and can lead to serious consequences for human beings and ecosystems.

The contribution of human CO₂ emissions as green-house gas in the climate change has been shown by studies such as [38]. The underground sequestration of the CO₂ produced from localized sources like power-plants and oil and gas recovery sites is proposed as a possible solution to reduce the rate of CO₂ emission into the atmosphere [13, 37]. The required technology for this solution is close to what is in use in the oil, gas, and mining industry. However, there are some challenges that are specific to carbon storage operations. Primary, the time and space scales in these problems are larger. Secondary, the risk of leakage of stored CO₂ up to the surface via conductive features like fractures and faults and man-made features such as leakage through ill-plugged wells and broken cap-rock due to high pressure imposed to the system during the injection operations is a major concern.

The main objectives of carbon storage operations are to maximize the storage size and the volumetric injection rate, and to minimize the risk of leakage of the stored CO₂. The CO₂ storage operations require a multidisciplinary collaborations. The work-flow from initial phases of a project until end of storage operations are divided between government and private section, research organizations and industry. It is the task of research community to investigate the safety of CO₂ sequestration and provide the methodology for CO₂ fate prediction [7].

Bachu [7] discusses the road-map of site selection for geological CO₂ sequestration. He defines the process in three steps: to assess the general suitability of the site, to perform the inventory study on the source point and storage location and the operational transport issues, and finally to investigate the safety and assess the capacity of the storage. Issues about safety and storage capacity are looked at differently from the perspective of immediate and ultimate results. For example, when talking about the risk of leakage, we might consider the leakage through ill-plugged wells or fractures during the injection time as the immediate risk. On the other hand, leakage caused by plume migration long time after the injection and contamination to other aquifer systems are considered as ultimated risks.

To predict the CO₂ injection fate, it is crucial to study the dynamics of flow in the medium. Dynamical study of flow includes quantification of acting forces in a geological heterogeneous medium that can end up in solving a complicated system of mathematical equations. It seems convenient to replace the geological heterogeneous medium with an equivalent homogeneous medium. However, proper modeling of geological heterogeneity is a major control on reservoir assessment and carbon storage studies [8, 21, 51, 52].

In this thesis, we report a series of works performed within a PhD program framework under MatMora project. MatMora is a strategic project that is defined to address the needs of mathematical tools to model the geological storage of CO₂ and to assess the uncertainty and risk in the modeling work-flow. The work in this thesis is focusing on the fundamental uncertainty in geological description used in modeling of CO₂ storage problems. The work is reported in a series of papers, and the objective is to perform a sensitivity analysis on variational geological parameters used to describe the geology of shallow-marine depositional systems. Although the focus is on a particular depositional system, the procedure can be implemented for any other systems of interest.

We start the introduction section by discussing the global warming and its causes, and the carbon storage as an interim proposed solution to mitigate the increasing level of industrial CO₂ emission to the

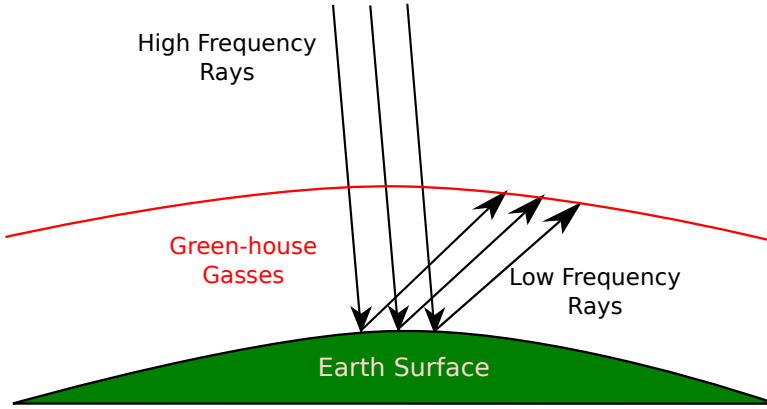


Figure 1.1: Green-house gases act like a blanket trapping the heat received from the sun.

atmosphere. Section 1.3 provides the work-flow of the works reported in the thesis. A brief overview of the literature is given and the work is discussed in that section.

In Section ??, we review a systematic definition for uncertainty from the literature and after that, the geological uncertainty and parameters are described. Flow equations for single-phase and two-phase flow problems are discussed in Section 1.6. In section 1.7, various flow regimes occurring during geological storage of CO₂ are described briefly by discussing the force balance within the medium at different times. Next we discuss the vertical averaging method which can be used in large aquifers to enhance the speed of simulation.

The introduction to the thesis continues by a discussion on flow simulation scenario and assumptions taken in the work in Section 1.9. We use a set of flow responses that monitor the performance of the operation and requirements to achieve the objectives of a typical carbon storage problem, with a special emphasis on the injection and early migration of CO₂ in the medium. Flow dynamics and a linear sensitivity analysis performed on the simulation results are discussed in this section.

Section 1.10 provides an overview on the fast flow solution techniques that can be used for rapid flow simulation. We use a response surface method to simulate the flow responses. This proxy model is then used in global sensitivity analysis and Monte-Carlo risk assessment process. The introduction section ends by introducing the Matlab functions used in the calculation work-flow.

1.2 Carbon storage

There are a number of theories that explain the causes of climate change. Milankovich theory [30] relates the energy received from the sun to the cyclical variation of earth orbit around the sun, and earth rotation around its axis. The earth orbit changes eccentricity between circular and elliptical. This influences the difference between earth and sun, and on its maximum influence can lead to about 20% difference in the energy received from the sun. The second variation occurs in the rotation of earth around its plane axis. This rotation wobbles approximately every 13600 years and the summer solstice switches from June to January. Also, a tilt variation of earth rotational axis happens approximately after every 41000 years. This can cause warmer winters and colder summers in high latitudes [30].

The solar radiation changes by a small amount of 0.1% over a 11 year cycle. Also on the scales of tens to thousands of years variations in the earth orbit result in seasonal changes and that in the past caused glacial and inter-glacial cycles.

The theory of green house effect relates the earth climatic change to the fact that the long wave radiation from earth back to atmosphere is absorbed by the green-house gases, mainly carbon dioxide, water vapor, and methane existing in the atmosphere. This results in trapping of heat energy and an increase in atmosphere temperature level (Figure 1.1) [30].

Human manipulations in the nature has led to about 100 ppm increase in carbon dioxide level in

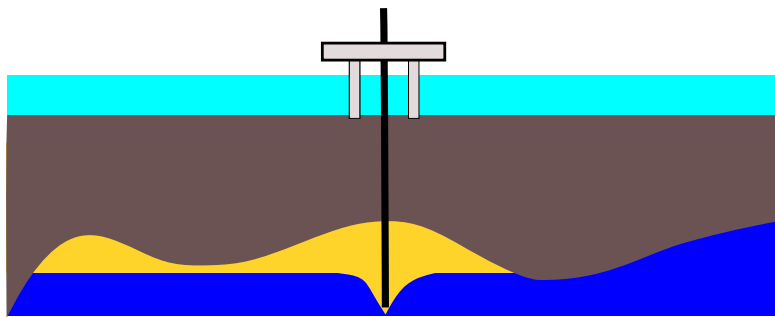


Figure 1.2: Geological sequestration is a proposed solution for mitigating the industrial CO₂ emissions.

the atmosphere. Most scientists believe that we are already experiencing the global warming due to green house effects. The IPCC Second Assessment report states that the climate change in the late 19th century is most likely due to anthropogenic causes.

Carbon capture and storage (CCS) has got a major attention in the industry and the scientific communities. According to the International Energy Agency (IEA), the cost of mitigating climate change by 2050 is estimated to be 70% higher without implementing CCS.

CCS is considered as an interim solution, because it is valid due to fossil fuel consumption, and the long term strategy of replacing fossil fuel with renewable energy will terminate the validity CCS. Therefore, initiating the CCS topic has to be done in a reasonable fashion such that it does not slow down the research for renewable energy. Another concern regarding the CCS is the acceleration of coal and fossil fuel consumption with the excuse of availability of CCS technology.

Sequestration of CO₂ at the ocean floor and also in deep underground aquifers are the options available for permanent storage of CO₂. Large availability of storage places and potential for almost permanent storage makes the geological sequestration the most practical option (Figure 1.2). Nevertheless, this alternative is not free from economical, social and industrial concerns.

In the last decades, the scientific community has been putting efforts into convincing the public about feasibility of these operations. A fair public acceptance must be based on social awareness. Any plan to increase the acceptance level in a society starts by measuring the current knowledge level of that society.

The EU has conducted a survey to assess the public awareness in 12 European states. This survey is published in the recent Eurobarometer report in May 2011. People's awareness and acceptance of climate change and its causes, and the methods to avoid or mitigate the problems, in particular the CCS technology, was examined in the survey. The majority of European participants are either fairly or very well informed about causes and consequences of climate change. However, the awareness of CCS in between the European respondents was low. Two third of the participants in the survey have had not heard at all about CCS.

The same survey suggests that the overall trust in Europe in the sources of information regarding CCS is best in universities and other scientific institutions. Governments are investing in research, not only to move toward industrialization of CCS, but also to make it well received by public. This highlights the importance of researching the storage of CO₂ and the way it is needed both for industrial demands and social concerns.

1.3 Modeling procedure

Predicting the fate of CO₂ storage involves identification and quantification of the relevant uncertainties and risk assessment process. The procedure starts with a geological description and continues with modeling of flow in geological formations. After constructing a deterministic flow model, the stochastic

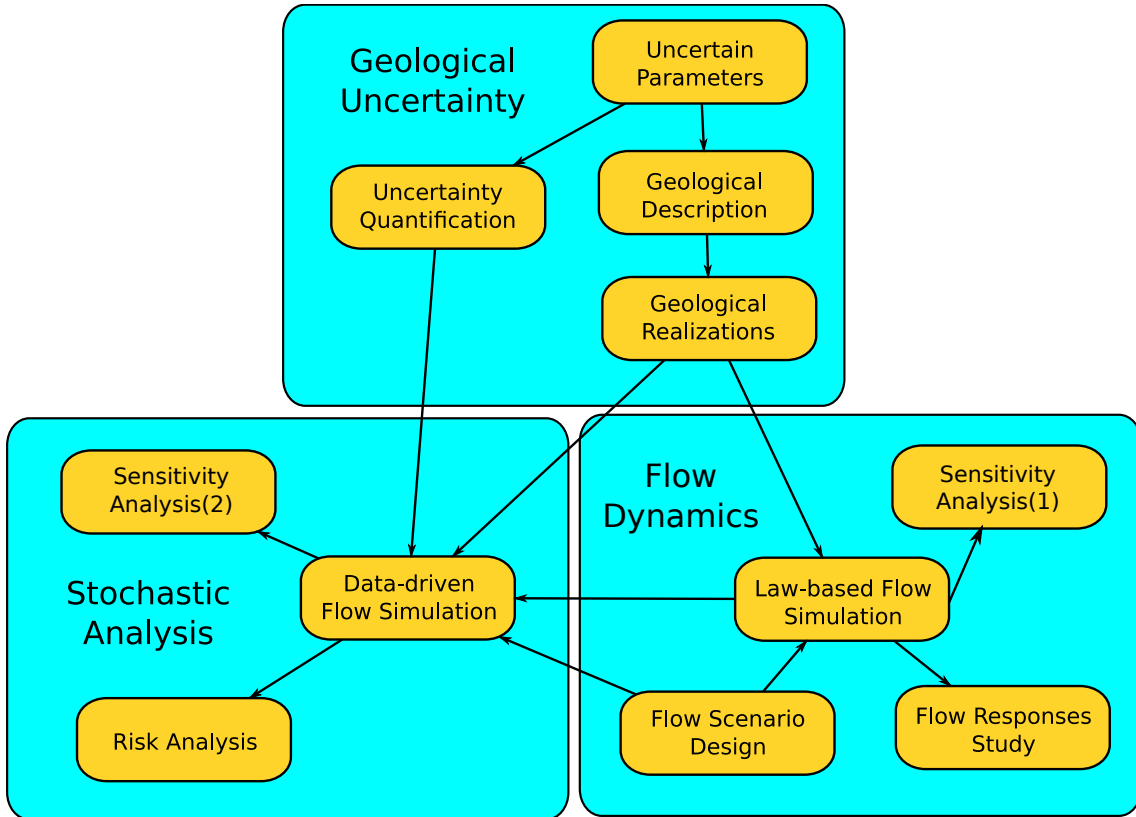


Figure 1.3: Modeling procedure diagram.

nature of the problem is analyzed by studying the variation in the model outcome due to uncertainties in the system.

Figure 1.3 shows the modeling work-flow implemented in the work of this thesis. The steps are categorized in three parts: geological uncertainty, flow dynamics, and stochastic analysis. The relations between steps are plotted by arrows in the flow-chart. In this section, we briefly describe each step. More details will follow in the next sections.

Uncertain parameters: In the first step, we identify the uncertain parameters of the model to study their influence in the modeling outcome. It is possible that our knowledge of model sensitivity to the parameters is limited. Then, in a conservative approach we choose larger number of parameters and by doing a primary sensitivity analysis with a fast technique, we filter out the important parameters. Herein, the focus is on the geological parameters. In addition, we use most of the influential parameters modeled in the SAIGUP study.

Uncertainty quantification: After identification of the uncertain geological parameters, we assign a likelihood to each of the parameters. It is hardly possible to have a unique likelihood template that applies to every geological location. Thus, we note that probabilities of existence for an uncertain geological feature can change from place to place. The uncertainty enters the modeling in the form of parameter frequency histograms. The conventional practice is to consider an analytical distribution function to be assigned to the parameters. However, the sampling procedure normally ends in scarce frequency histograms that are difficult to fit into a unique analytical distribution function.

Geological description: Geological uncertainty study is normally done by series of runs to measure the sensitivity of the model to the parameter variations. Results are valid, only if the geology used in the work-flow is representative of reality. The process of geological description results in a large number of realizations to be used in the next steps of the study.

Flow scenario design: Herein we define the initial and boundary conditions of the CO₂ injection problem. Also, we specify the injection scenarios. Possible simplifying physical assumptions will be

taken here. Each scenario is implemented in all geological realizations.

Law-based flow modeling: After defining the injection problem, we simulate the flow dynamics in the chosen realizations. We use a two-phase flow model and a standard commercial simulator.

Data-driven flow modeling: Modeling the flow dynamics via formulations of physical laws normally results in complicated equations with large degrees of freedom. The computational cost of solving these equations is high, in particular if these models are used for uncertainty related studies that require a large number of simulations to cover the variation in the uncertain parameters.

The so called data-driven methods, are mathematical functions that are specified by correlating a set of unknown flow attributes to their corresponding uncertain parameter values. These methods need to be tuned by a law-based method before employment. Because these methods are designed to be only dependent on the uncertain parameters, they are normally low in computational costs. However, they may exhibit the pitfall of not following the physical rules and in some cases produce unrealistic results.

Flow responses study: Once the simulation results are obtained from the flow modeling procedure, it is possible to calculate the important flow responses from simulation results. The fate of carbon storage and assessment of the operations can be inferred from these responses. Storage volume capacity and rate, and leakage risk are evaluated from flow responses. Responses include pressure distribution over time, CO₂ plume development, and other quantities describing the dynamics of flow in aquifer.

Sensitivity and risk analysis: The sensitivity analysis is performed in two ways: firstly by using three dimensional two-phase flow simulations on all realizations available for demonstrating the geological variability and via a linear gradient method. In the second method, we employ an approximating polynomial to perform global sensitivity analysis and stochastic uncertainty studies. Using the relatively fast data-driven method, we perform a Monte-Carlo process on 10000 simulation cases.

1.4 Uncertainty Sources

Sources of uncertainty can exist in every part of CO₂ storage modeling process. Herein, we briefly describe each of the possible contributions to the uncertainty in modeling within various parts.

Uncertainty in physical modeling: We might ignore some phenomena during the physical modeling of CO₂ storage that can be influential in the flow behavior. This might happen due to lack of awareness of the phenomena or by underestimating the significance of it. For example, we might ignore the heat exchange within the system, assuming that heat transfer does not play an important role in the flow performance. If some parameters in the modeling are sensitive to the heat and change by temperature variations, the assumption to ignore heat transfer effect will introduce considerable uncertainty in the outcome of the modeling.

Mathematical formulation and numerical approximation: A specified physical problem can be formulated mathematically in more than one way. The choice of primary unknowns to be found can change the mathematical form and nature of the equations. Degrees of non-linearity and coupling between unknowns in the equations can vary in different formulations.

Modeling CO₂ injection and migration in a realistic geological formation results in a complicated mathematical system that in most of the cases can not be solved analytically. The numerical approach to approximate the original mathematical system, normally introduces errors in approximation. Mathematical analysis can help in estimating the error or its order, but it might not be doable for complicated models.

Geological uncertainty: The high costs of data acquisition and technical limitations introduce a huge amount of geological uncertainties in CO₂ storage modeling. The injected CO₂ may travel in a large spatial scale and providing enough geological information and the medium attributes is a big challenge.

User introduced uncertainty: These type of uncertainties are caused by the errors introduced by a user for her/his biased choice of modeling tools and interpretations of modeling results.

1.5 Geological modeling

The central part of a successful CO₂ storage fate modeling is to provide plenary aquifer models that depict the geological heterogeneity in a realistic manner. This requires having an inclusive understanding about model sensitivity with respect to different geological parameters and quantifications of geological uncertainty and its impacts on the process.

The conventional practice of geological modeling includes using geostatistical models. It is possible that two different heterogeneity patterns produce the same geostatistical model, as discussed by Caers [14]. Therefore, a geostatistical model does not represent a unique reservoir image and if we do not include additive information in the process, we might end-up with an unrealistic heterogeneity texture[14, 21]. The primary attention in our work has been on this issue and to provide a more realistic way of geological uncertainty analysis for CO₂ sequestration by including information of geological features and textures in the process.

1.5.1 Geological description

The geological storage of CO₂ requires large accommodation of subsurface volumes. Only sedimentary basins, which hold relative large pore volumes, are generally suitable for this mean. However, not all sedimentary basins are similarly appropriate for CO₂ sequestration.

Convergent basins along active tectonic areas pose a higher risk of CO₂ leakage due to volcanism, earthquakes, and active faultings. Divergent basins located on the stable lithosphere are much less prone to earthquakes or other catastrophic event that can lead to accidental releases of large CO₂ quantities. Therefore, specific considerations must be done in selecting injecting site locations with respect to security of subsurface storage.

Sedimentary basins are composed of various lithological facies. Stratigraphic architecture and sandbody geometry control the capacity and effectiveness of CO₂ sequestration. As a result of various tectonic depositional and erosional process, low and high permeability rocks are accumulated on top of each other that can form stratigraphic flowpath leading to various directions and speed of subsurface flow. Three types of formations can be characterized: aquifers, aquitards, and aquiclude.

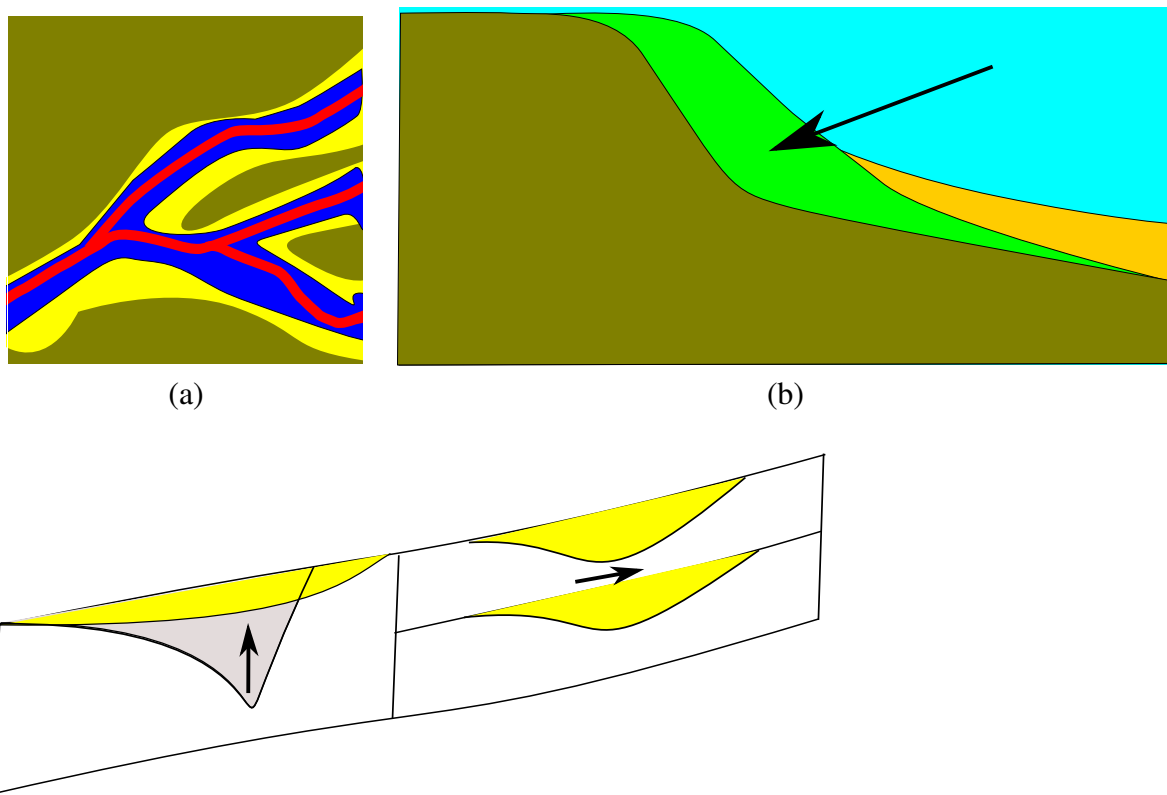
Aquifers are high permeability strata that provide major beddings for flow transport. Good rock quality in continuous sandbodies allow for efficient CO₂ storage in an acceptable capacity volumes. Aquitards are made of low permeability strata that provide beddings with orders of magnitude slower flow than aquifers. Layers of aquifers and aquitards are formed by thick accumulation of sediments that undergo burial, compaction, lithification and uplift over millions of years. They can be covered by aquiclude, which are evaporitic beds that are impervious to fluid flow.

Typical seal rocks include, from most ductile to most brittle : salt, anhydrite, hydrogen-rich shales, dense mudstone, tightly cemented sandstones, anhydrite-filled dolomite, carbonate, or silica-cemented sandstones, and cherts REF.

Aquifer pressure is normally close to hydrostatic, because of the conductivity within the medium that allows for pressure equilibrium over long time. High pressurized compartments can exist in highly sealed structures. The pressure of the sedimentary basin have a significant impact on its suitability for CO₂ storage REF. trapping mechanism for CO₂ is in two main parts: stratigraphic and structural traps. Stratigraphic trapping is primarily controlled by the geometry of depositional facies and sand body continuity. These factors control the permeability distribution within the medium that controls the efficiency of injection and storage of CO₂.

Structural heterogeneity factors include faults, folds, and fracture intensity. the dip angle of formation layers control the buoyancy forces applying on CO₂ plume migrating along the conductive layer. Fractures can enhance the mobility of the plume and sealing faults can provide structural traps for long term CO₂ storage. Anticline structures also can be a permanent trap for stored CO₂.

Depositional environment varies between fluvial to marine systems. The texture and degree of sandiness of beach deposits are a function of the shore profile, typically consisting of a gently sloping



formation layering in a transition from near shore to deep offshore. Deposits range from sandy, coarse grain structure near the shore, to muddy, burrowed, fine grained sand in the lower off shore. High energy near the shore that is a result of interplay between wave, fluvial, and tidal forces, filters out the larger grains in the deposition.

Therefor, near the shore contains large continuous sand bodies that have good quality rock. This is the reason for shallow-marine systems to be appropriate trap for hydrocarbons and analogeously, good candidates for CO₂storage.

The beach facies normally are homogeneous rocks with internal heterogeneity due to tidal systems. In contrast, mixed-load fluvial that contain both mud and sand are more heterogeneous than beach systems. The presence of numerous mud drapes as a result of periodic floods, serve as barriers to fluid flow. Heterogeneity in the fluvial systems exist in multiscale levels, from small scale variations of rock type near the river bed, to the large scale heterogeneity in fluvial channel fill sandstones and over-bank deposits. Heterogeneity also occurs within these systems in the form of muddy abandoned channel fill deposits.

In theory, we prefer a medium that allows for more lateral movement to overcome the buoyancy bypassing of the flow. Heterogeneity in the vertical direction, such as shales inter-bed barriers can serve for this and disperse the flow in the lateral direction. Structural heterogeneities can have a similar impact. In addition, splitting a large plume into smaller plumes lowers the risk of leakage of huge CO₂amounts via potential breakings in the integrity of the sealing barriers, or abandoned wells.

CO₂injectivity is related to sequestration capacity and effectiveness, and can be defined by the conductive cross sectional area. Stratigraphic factors that enhance injectivity are high permeability and injection interval thickness. In addition, the lateral permeability architecture can influence the injectivity quality. The lower the injectivity is, the higher will be the pressure buildup in the medium due to injection.

Over the last two decades, there have been a large number of studies concerning the subsurface storage of CO₂. Several authors investigate the efficiency of geological CO₂storage based on regional data in a specific site location.

A case study from the Texas Gulf Coast investigates the susequestration capacity and efficiency in

accordance to the geological heterogeneity. The study performs a site-scale assessment of applicability of geological sequestration in brine formation. Injection is considered in the Frio formation which is a sandstone-rich, high quality, overlain by a thick, regionally extensive shale in the upper Texas Gulf Coast. Migration of CO₂ during injection (20 years), and post-injection (40 years) is studied within different heterogeneities represented by stochastic modeling of geological sediment via petrophysical parameters. Structural heterogeneity is modeled by layers dip angle and faults at different locations. Six models are made based on regional available geological information.

The study shows that in a homogeneous rock volume, CO₂ flow paths are dominated by buoyancy, bypassing much of the lateral rock volume. If the permeable rock is interbedded with multiple low permeability layers, the flow paths are dispersed, enhancing the lateral movements of CO₂ allowing for larger percentage of contact with rock volume. The study suggests that dip angle enhances buoyancy forces and decreases storage capacity, while compartmentalization by faulting appears to increase sequestration capacity at the cost of increased pressure, and consequently, increased risk of CO₂ leakage.

A number of pilot sites are established worldwide to test the large scale injection of CO₂ in the subsurface formation. The In Salah project in Algeria is an industrial-scale injection project into a fracture-influenced, matrix-dominated sandstone formation. The reservoir matrix comprises tidal deltaic sandstone. The project benefits from relatively high level of data acquisition: wireline and LWD well logs, image logs and production and geophysical monitoring. In addition, most valuable monitoring method has been the usage of satellite air-borne radar above the injection well. Also, chemical tracers are used in the injected CO₂ to differentiate the natural CO₂ in place from the injected volumes, when the CO₂ breaks through other wells.

The detailed analysis highlights the geological controls on the movement and dispersion of CO₂ plumes. The injection is performed via a horizontal well perpendicular to the geomechanical stress field and the faults presenting in the domain. This, along with the fracture network, enhance the plume migration- about three times faster than the flow in a homogeneous domain.

Results from In Salah illustrate the value of reducing geological uncertainty by employing sufficient logging tools and monitoring techniques.

CO₂-SINK project at Ketzin Germany, is another pilot site for practicing subsurface CO₂ injection. The injection is performed in the Stuttgart formation that is geologically heterogeneous within an anticline structure. The Stuttgart formation is made of sandy channel facies of good rock quality alternate with muddy flood-plain-facies. A thick cap-rock section covers the Stuttgart formation.

Practically, including all details of every scale into flow simulation model is impossible. Various simplifications have been made to account for heterogeneities in modeling. Some earlier studies consider two dimensional modeling, with homogeneous or geostatistically populated permeabilities. The study in [?] simulates an escape rate of CO₂ in a homogeneous medium similar to Utsira formation in Norway. By changing the horizontal permeability, they emphasize that the permeability of the layer beneath the cap-rock (where most of CO₂ injected volume accumulate due to buoyancy forces), plays an influential role in the CO₂ migration process. However, this study assumes no vertical heterogeneities. A layered heterogeneity is examined in [68]. They used a log normal distribution of permeability in a simplified two dimensional grid to account for viscous and gravity forces. Results suggest that the sweep efficiency of CO₂ in the porous medium is low, and heterogeneity, in particular the vertical transmissibility, can have a big impact on the storage efficiency.

To examine the impact that the geological heterogeneity degree can have on the CO₂ sequestration modeling, [28] constructed a suite of three dimensional simulation models, with varying net to gross ratios. A radial variogram, with a shale length of 300 m, was used to populate five models of varying degrees of net-sand-to-gross-shale ratios. The models were up-scaled, using flow-based methods, to make the computation feasible. The study concludes that formations containing shale barriers are effective in containing an injected CO₂ plume within the formation and that heterogeneity serves to limit the reliance of the formation seal as the only mechanism for containment.

1.5.2 Geological parameters

From the flow modeling perspective, sources of geological uncertainty can manifest themselves in the rock parameters that go in the flow equation such as permeability and porosity. To represent the geological uncertainty, it is not enough to randomize these parameters. This approach might work in simple geological models, but it can fail to give plausible results in the realistic heterogeneous problems with uncertain structural and depositional descriptions.

In response to the EU priorities of reducing time to first oil and of improving overall hydrocarbon recovery efficiency, the interdisciplinary SAIGUP study was initiated to increase the understanding of the influence of geological uncertainties in oil field recoveries. SAIGUP stands for 'sensitivity analysis of the impact of geological uncertainties on production forecasting in clastic hydrocarbon reservoirs'. The context in SAIGUP is defined for shallow-marine depositional systems. The main objective of the SAIGUP project has been to perform a quantitative sensitivity analysis to measure the impact of sedimentological and structural variations within geological descriptions on oilfield recovery estimates [39, 47, 49].

Six different rock types are considered in the geological modeling. The rock properties within each facies are populated based on real data. Variations are considered in a horizontal-vertical matrix in three levels of heterogeneities, low, medium, and high, as illustrated in Figure ???. The design focused on special considerations. For example, making complex enough heterogeneities to be a plausible representative of realistic models, and producing large enough number of realizations with sufficient overlapping to be able to perform a quantitative sensitivity analysis.

Sedimentological variability is modeled in small and large scales and combined to provide realistic variations of reservoir heterogeneities. All models are considered in a progradational sedimentary environment. A regular grid is used for all of the realizations and the total bulk volume is the same in all cases. Each geological realization contains about 1.5 million cells in the fine model. Figure 1.4 shows the fine grid model for a selected realization with medium level of heterogeneity. A major fault in the model breaks the structure and makes large vertical depth difference in the two parts of the model (from about 1500 m to 3000 m). Thickness of the model is much smaller than these depth differences. In order to see the property variations on the grid in the vertical direction, we map the properties on a flat uniform geometry (Figure 1.5).

Figure 1.6 shows the spatial distribution of the six modelled facies in the selected realization, and Figure 1.7 shows the histogram of lateral transmissibility within each facies and the total model in the logarithm scale.

Structural aspects are modeled via fault modeling within geological description. Faults are considered in different levels of intensity, orientation, and transmissibility.

Although these models were designed to study the impact of geological heterogeneity on oil recovery, they may also be used to model a scenario in which CO₂ is injected into an abandoned reservoir. Therefore, we have selected five parameters from the setup and varied these parameters by combining different levels for our CO₂ storage study. These features are lobosity, barriers, aggradation angle, progradation, and fault. In the following, we describe each feature briefly.

Lobosity: Lobosity is a metric for describing the interplay between fluvial and wave processes in a shallow-marine depositional system. As the river enters the mouth of the sea, the shore-line shapes where the river flux crash with the waves from sea. The balance between the sediment supply from rivers and the available accommodation space in the shallow sea defines the shore-line shape. Sea waves smear out the shore-line, while fluvial flux from river makes branches into the sea. Less wave effect produces more pronounced lobe shapes around the river entrance into the sea.

The channels made into the sea mouth by fluvial supplies contain good quality rocks with relatively higher porosity and permeability and poor quality rock types are located between the conductive branches. Reservoir quality decreases with distance from the shore-face. Lobosity variation can influence the CO₂ injection operation and plume distribution in the aquifer. In this study, models of three levels of lobosity are used: flat shoreline, one lobe and two lobes, see Fig. 1.9.

Barriers: Barriers are mud-draped surfaces sitting between reservoir sections that are caused by

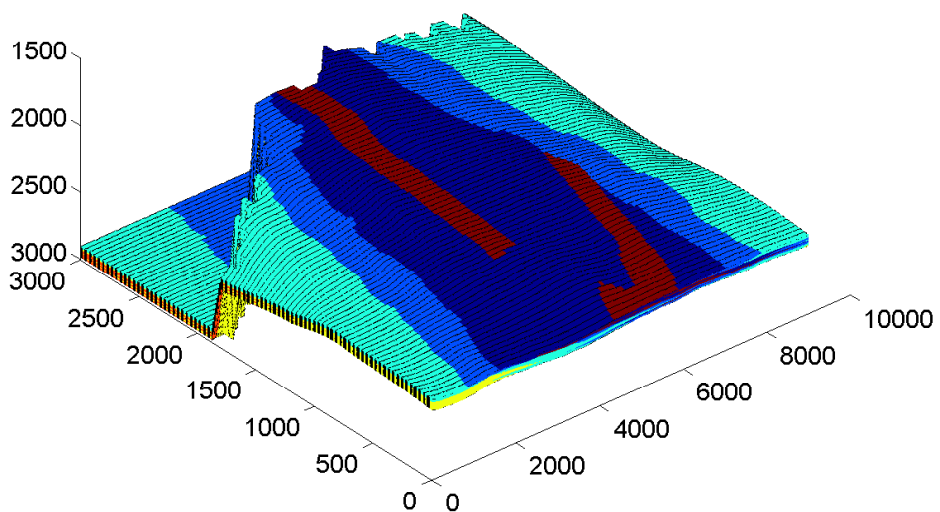
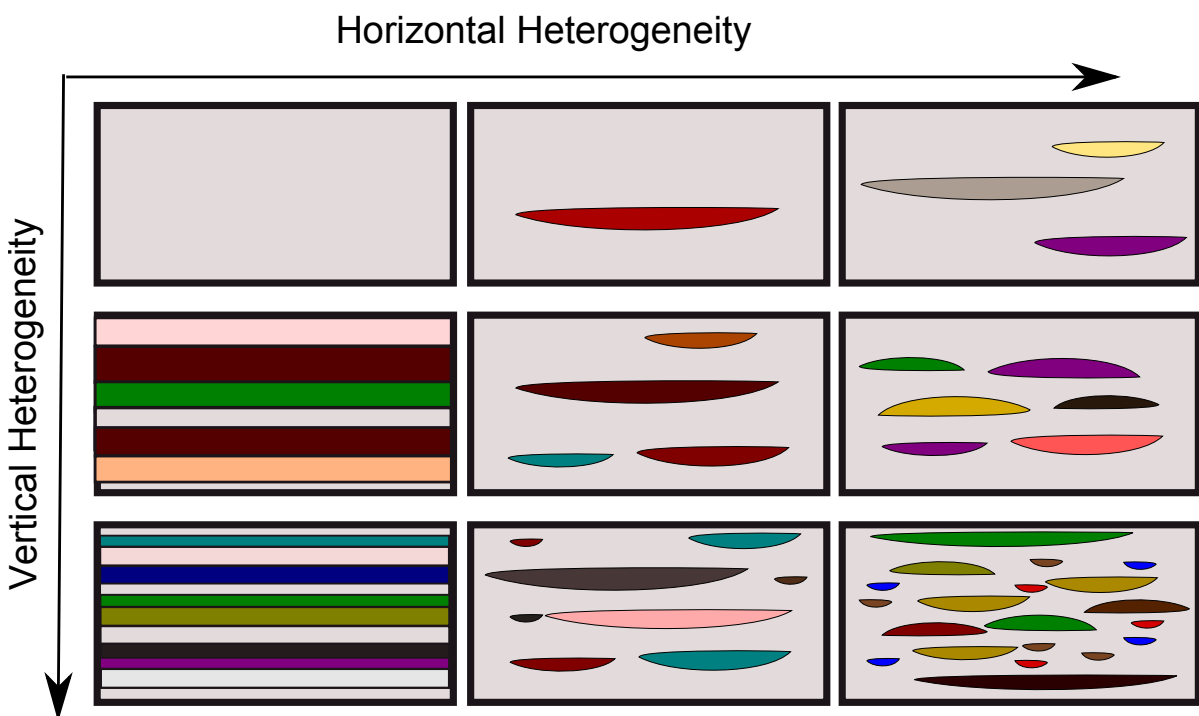


Figure 1.4: bla bla bla

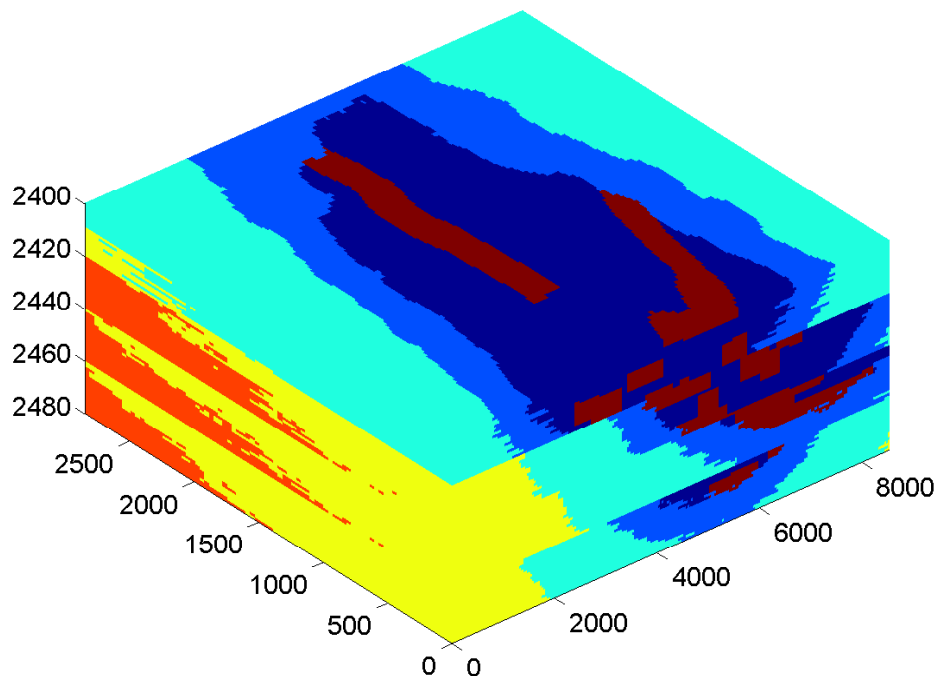


Figure 1.5: bla bla bla

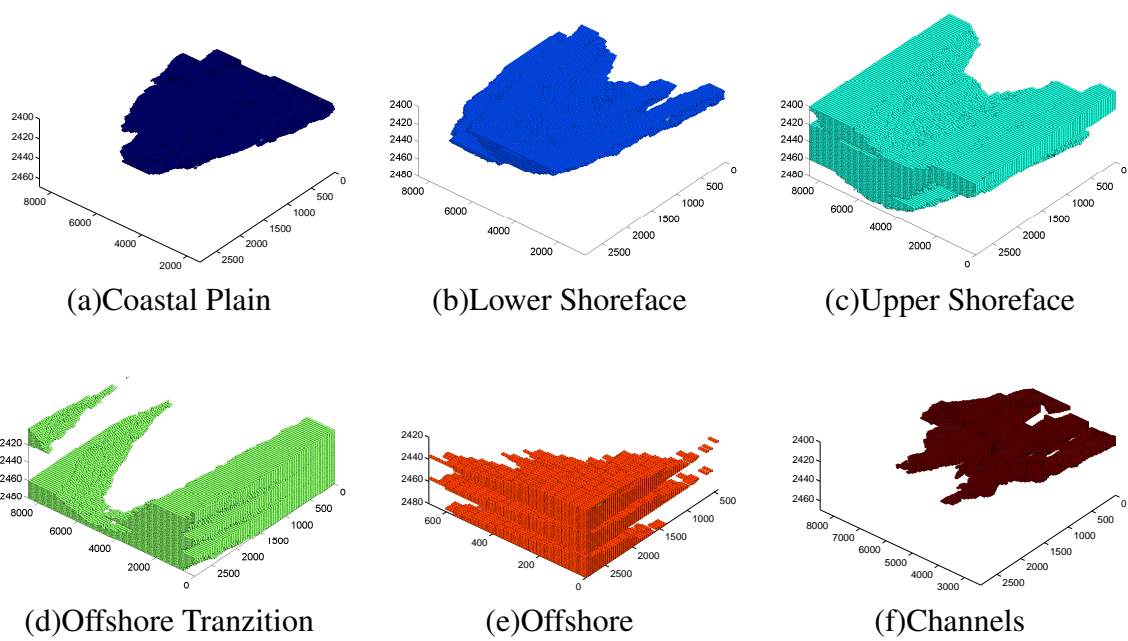


Figure 1.6: bla bla bla

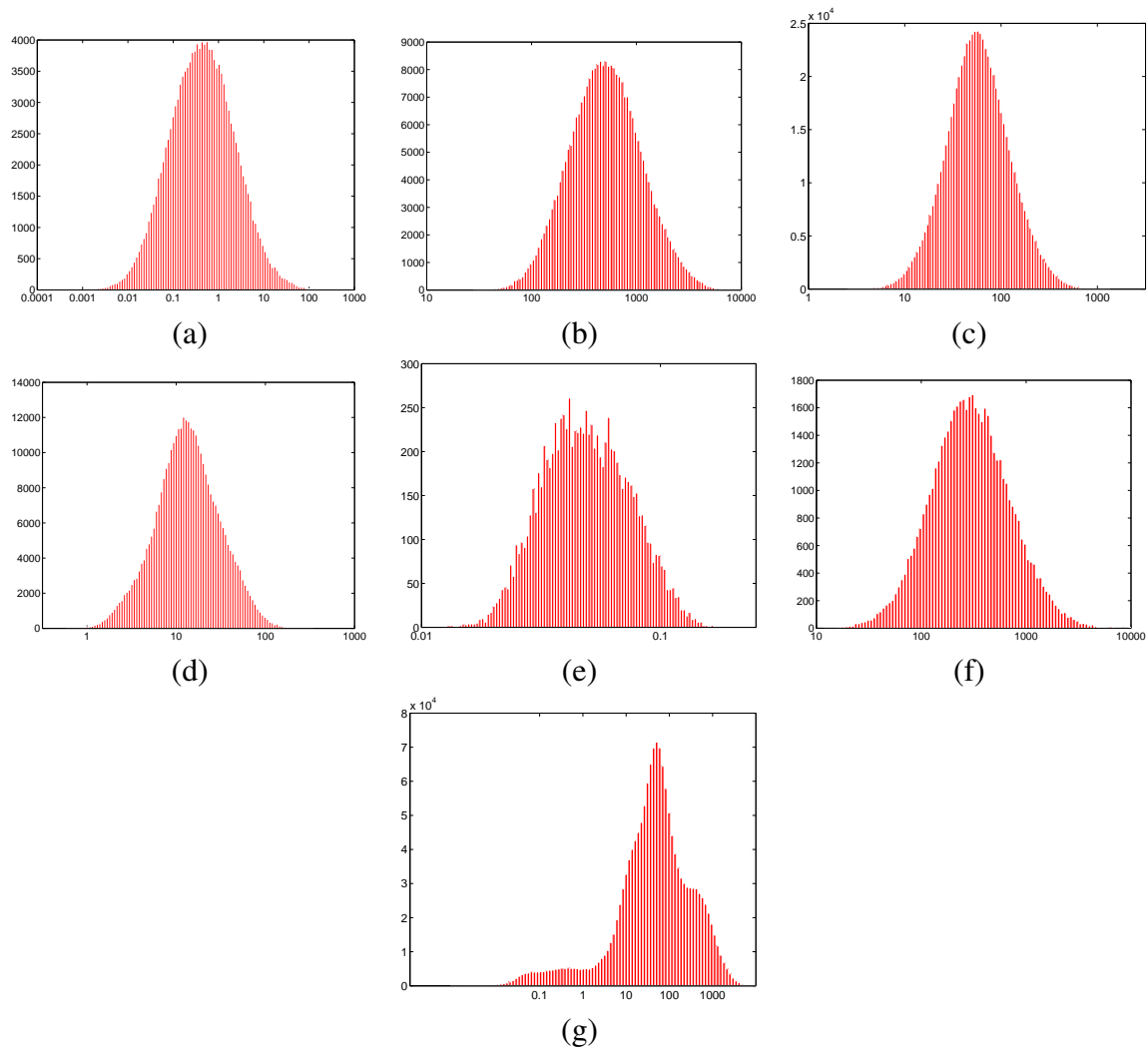


Figure 1.7: bla bla bla

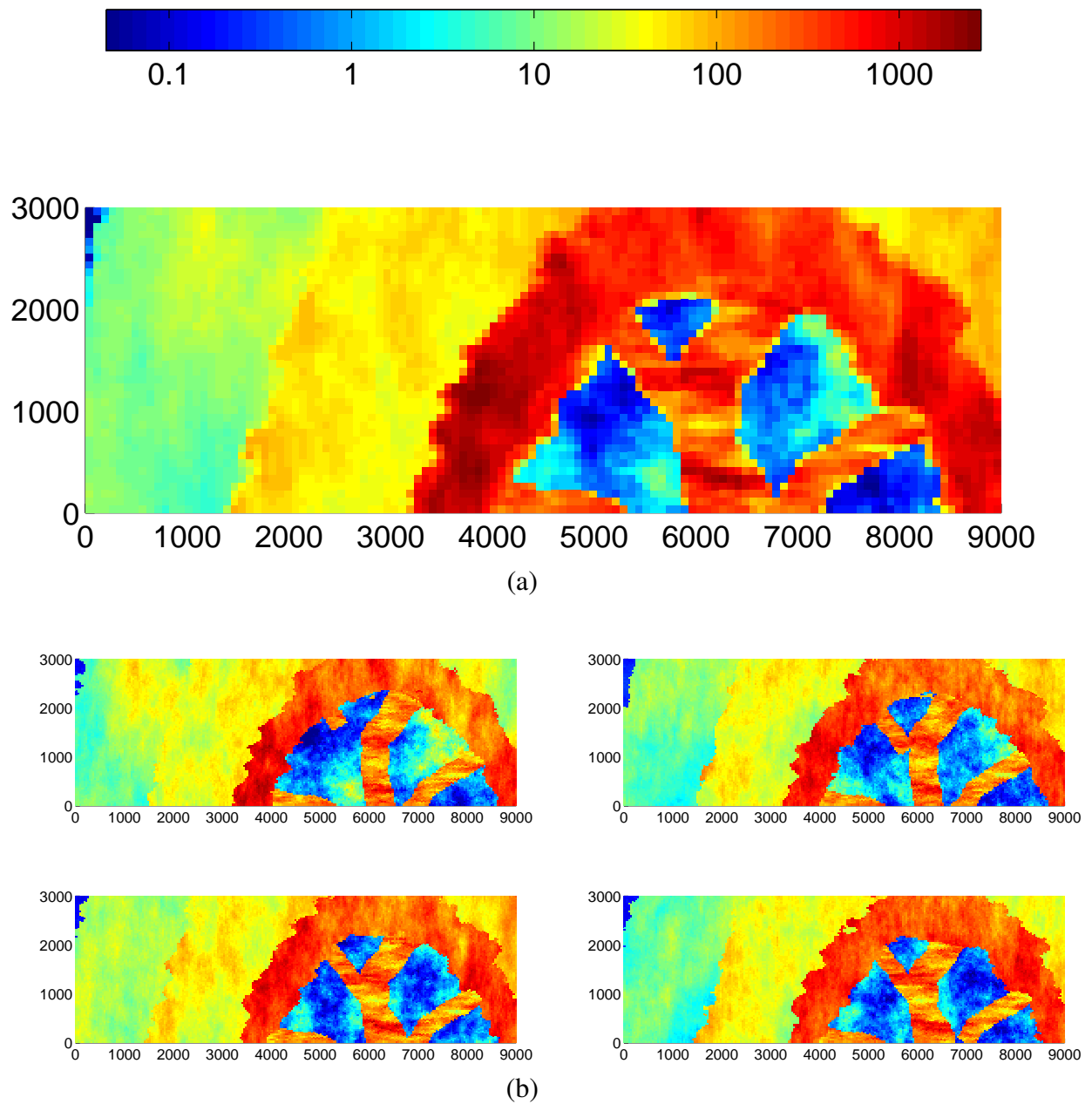


Figure 1.8: bla bla bla

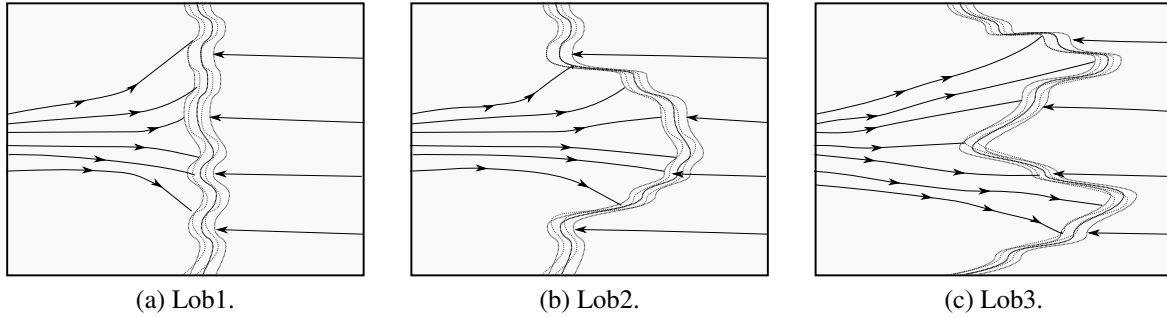


Figure 1.9: Lobosity levels are defined based on the shoreline shape, which is caused by the interplay between fluvial and wave forces.

periodic floods in a shallow-marine depositional system. Barriers extend in both vertical and lateral directions and are potential significant barriers to flow. In the SAIGUP domain used here, these barriers were modeled by defining areas between layers with zero transmissibility multipliers. The areal coverage designed in three levels: low (10%), medium (50%), and high (90%). We use the same variations in this study, see Fig. 1.10.

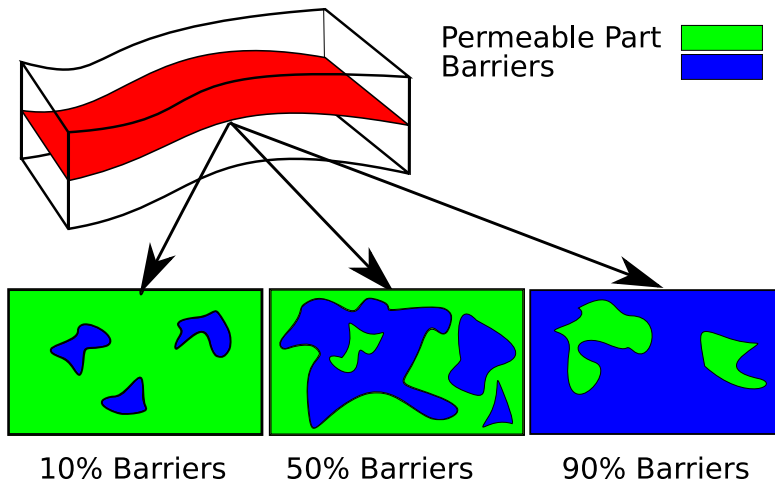


Figure 1.10: Barrier levels caused by periodic floods.

Aggradation angle: In shallow-marine systems, the sediment supply from rivers deposits in a spectrum of large size grains in the land side toward fine grains deep in the basin. Amount of deposition supplied by the river compared to the accommodation space that the sea provides defines the transition of different rock-types between the river and the sea. If the river flux or sea level fluctuates, the equilibrium changes into a new bedding shape based on the balance of these factors.

When the river flux increases, it shifts the whole depositional system into the sea causing an angle between transitional deposits that are stacked on each other because of this shifting. This angle is called aggradation angle. Three levels of aggradation are modeled here: low, medium and high (Fig. 1.11). As we will see later, aggradation can have a major role in influencing the CO₂ flow direction in the medium.

Progradation: Progradation is the depositional-dip direction between the sea and the river. Two types are considered here: up and down the dominant structural dip. Progradation combined with lobosity can influence the plume development in the medium, as the injected CO₂ plume migrates upward to the crest goes through heterogeneities (Fig. 1.12).

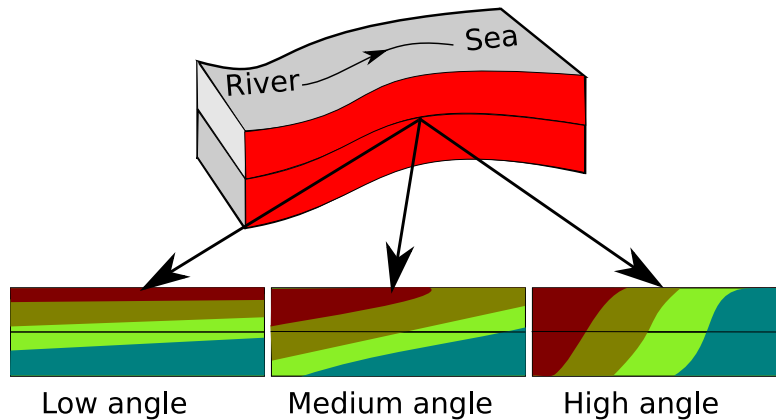


Figure 1.11: Aggradation angle levels.

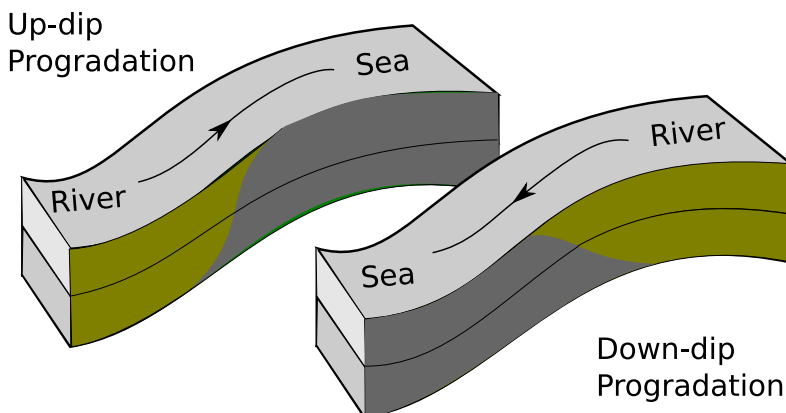


Figure 1.12: Progradation levels.

1.6 Flow equations

After introducing the parameters that make our geological model, we need to define the flow problem. In this section we discuss various formulations of the governing equations describing single and two phase flow in porous medium. We introduce the functionalities and auxiliary equations required to close the flow equation system. This section also includes a brief mathematical discussion on the flow equations. We discuss various flow regimes in the medium in the next section.

1.6.1 Single phase flow

Assume a porous domain Ω with boundary Γ as shown in Figure 1.13. We write the continuity equation in general form for a single phase flowing in the domain [1, 2, 15]:

$$\text{Accumulation} + \text{In-Out Flux} = \text{Source/Sink} \quad (1.1)$$

$$\int_{\Omega} \frac{\partial}{\partial t} (\phi \rho) d\tau + \int_{\Gamma} (\rho v \cdot n) d\sigma = \int_{\Omega} q d\tau \quad (1.2)$$

In Equation 1.4, ϕ is the rock porosity, ρ is the fluid density, v is the flow velocity, and n is the normal vector to the boundary. The term q denotes the mass source or sink in the system. Integrations are taken over arbitrary domain Ω with boundary Γ (Figure 1.13). Flow velocity is considered at the representative elementary volume (REV) scale for porous media [9].

The resistance of porous medium against flow results in a velocity which can be calculated from pressure and gravity gradient and fluid properties in the medium. This is governed by Darcy equation for single phase flow:

$$\mathbf{v} = -\frac{K}{\mu} \cdot (\nabla P + \nabla D). \quad (1.3)$$

In Equation 1.3, K is the permeability of the medium. Permeability is a function of pore size distribution and connectivity and in the macro scale, it is a measure of medium conductivity when a fluid is flowing through the medium (Figure 1.14). D is the gravity term that is a function of fluid specific gravity and elevation in vertical direction.

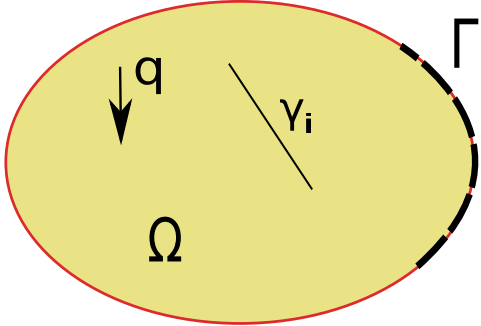


Figure 1.13: Flow domain and boundaries.

Substituting velocity term from Equation 1.3 into Equation 1.4 gives:

$$\int_{\Omega} \frac{\partial}{\partial t}(\phi\rho)d\tau - \int_{\Gamma} (\rho(\frac{K}{\mu} \cdot (\nabla P + \nabla D)) \cdot n)d\sigma = \int_{\Omega} qd\tau. \quad (1.4)$$

As a primary unknown in Equation 1.4, pressure depends upon boundary conditions as it is clear from the second term left hand side of Equation 1.4. Also, any geological discontinuities in the medium (γ_i in Figure 1.13) appear in Equation 1.4 through K tensor and can influence pressure behavior in the domain.

The second term in Equation 1.4 can be converted into an integration over domain Ω , using divergence theorem resulting in the following:

$$\int_{\Omega} [\frac{\partial}{\partial t}(\phi\rho) + \nabla \cdot (\rho v)]d\tau = \int_{\Omega} qd\tau. \quad (1.5)$$

Equation 1.5 is valid for arbitrary domain Ω , hence the equality is valid for the integrands *almost everywhere* in domain Ω in the *general* situation:

$$\frac{\partial}{\partial t}(\phi\rho) + \nabla \cdot (\rho v) = q. \quad (1.6)$$

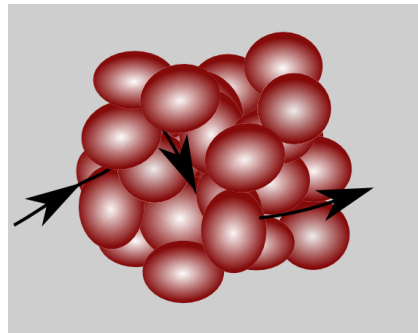


Figure 1.14: Permeability is an indication of how easy it is for the fluids to flow through the medium.

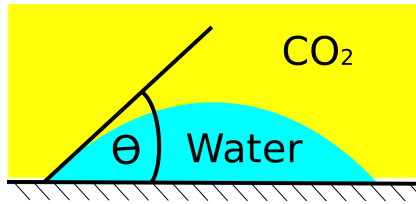


Figure 1.15: Wettability and interfacial tension in water-CO₂ system.

Fluid and rock change in volume with pressure variations. These dependencies are defined by a parameter called total compressibility, which is approximated by a combination of rock and fluid compressibilities:

$$C_T \approx C_{rock} + C_{fluid}, \quad (1.7)$$

where

$$C_{rock} = \frac{\partial \phi}{\partial P}, \quad (1.8)$$

and

$$C_{fluid} = \frac{1}{\rho} \frac{\partial \rho}{\partial P}. \quad (1.9)$$

In Equation 1.8, C_{rock} can be assumed constant in moderate pressure changes depicting a linear relation between pressure and porosity. Also, Equation 1.9 can be expanded resulting in the following [55]:

$$\rho = \rho_0 \left(\frac{P}{P_0} \right)^m \exp[C_{fluid}(P - P_0)]. \quad (1.10)$$

Assuming slight compression gives [64]:

$$\rho \simeq \rho_0 + C_{fluid} \rho_0 (P - P_0) \quad (1.11)$$

By substituting from Equations 1.7, 1.9, 1.8, and Equation 1.3 into Equation 1.6, density vanishes and by defining volumetric source/sink η , we have the single-phase diffusivity equation:

$$C_T \frac{\partial P}{\partial t} - \nabla \cdot \left[\frac{K}{\mu} (\nabla P - \nabla D) \right] = \eta. \quad (1.12)$$

1.6.2 Two-phase flow

In a two-phase flow of CO₂ and water within porous media, interactions between phases lead to loss of energy. This introduces specific phenomena occurring in the pore scale that have impact on the macro scale flow performance. More complicated equations appear in modeling the two-phase flow compared to the single-phase problem. First we describe some of the conceptual two-phase phenomena in the pore scale and then we will continue by deriving the flow equations for two phases in the system, i.e. CO₂ and water.

When CO₂ and water get in contact in the pore scale, an interface forms between them such that the energy in the system is minimized. Water and CO₂ are also in contact with the porous medium and the interface between them forms an angle from the solid phase in the water phase (shown by θ in Figure 1.15) that depends on their competence for wetting the rock. This is called wettability and the phase with the preference of wetting the solid phase is called the wetting phase. The other phase is called the non-wetting phase. Conventionally, θ is measured inside the denser fluid. If $\theta < \frac{\pi}{2}$ then the denser phase is the wetting phase. Wettability in a porous medium depends on the fluids and the rock. It can have a significant influence in the phase displacement within the medium. For water-CO₂ system, normally water is the wetting phase.

At very low water saturations, water covers the rock grains surface in layers that can go to the thickness size order of molecular films. In this situation the water phase is immobile and can not make

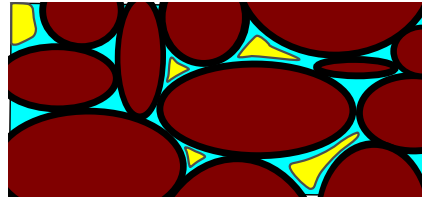


Figure 1.16: Multi-phase flow in the pore scale.

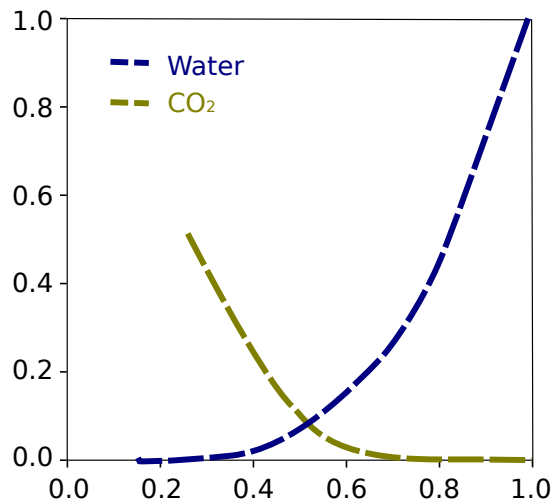


Figure 1.17: Two-phase flow and relative permeability.

a continuous phase moving through the porous medium. As water saturation in the medium increases, the layers covering the rock grains grow in size until the saturation exceeds a critical level, above which the water phase is able to flow in the medium. This saturation is called the critical or connate water saturation. In a water wet rock, once the critical water saturation is reached (for example, during the first deposition of sediments), it can not go below that level by being displaced via a non-wetting phase. Therefore, when we inject CO₂ into an aquifer, there will always be some residuals water saturation in the regions invaded by CO₂.

As a non-wetting phase, CO₂ flows in the middle part of the pore space as shown in Figure 1.16. If CO₂ saturation decreases in the medium, it reaches a critical level under which it can not make a continuous phase flowing through the pore-network. Tiny drops of CO₂ are trapped in the middle of the pore space and only very large pressure difference across the pore can move it out of the pore. This level of CO₂ saturation is called the residual saturation. Higher residual saturation is more interesting for the purpose of immobilizing more volumes of injected CO₂ in the aquifer, which reduces the risk of CO₂ leaking through any breakings in the geological formation and channeling toward surface.

Relative ease for the phase to flow within the medium is described by the relative permeability parameter. Relative permeability is a function of wettability and phase saturation. High phase saturation indicates a higher space available for the phase to flow through that space. A sample of CO₂-water relative permeability functions are shown in Figure 1.17. A library of relative permeability curves for CO₂-water system for various rock-types is available at [10].

The difference in surface tension between water and CO₂ causes a pressure acting on the interface of the two fluids. This pressure is called capillary pressure. In addition, capillary pressure depends on the geometry of pores. Since the pore geometry is very irregular, it is more convenient to use simpler geometry to drive the concept of capillary pressure. Therefore, experimental work in the laboratory is required to specify the capillary pressure functionality in a special case.

Assuming a geometry of pipe to represent a pore structure, after balancing the forces in the pore-system capillary pressure can be written in the following form:

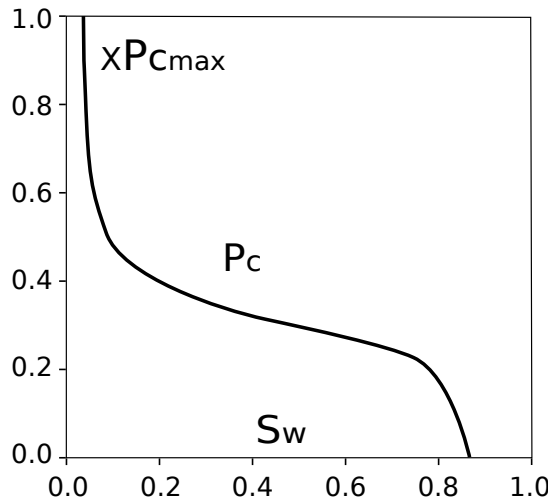


Figure 1.18: Capillary pressure can be expressed as a function of wetting saturation. The plot is a typical curve of capillary pressure function with a maximum of $P_{c\max}$

$$P_c = \frac{2\sigma}{r} \cos\theta, \quad (1.13)$$

where σ is the interfacial tension, θ is the angle between the interface and the solid phase, and r is the radius of the pore.

Capillary pressure is a jump in phase pressure across the interface of the two phases. Therefore, we can relate it to the phase pressures:

$$P_c = P_{nw} - P_w. \quad (1.14)$$

Here, P_{nw} is the non-wetting phase pressure and P_w is the wetting phase pressure.

Capillary pressure can be expressed in an empirical relation as a function of wetting phase saturation. Lower capillary pressure is expected for higher wetting saturations, and capillary pressure values go up for lower wetting saturations (Figure 1.18).

Assume hydrostatic equilibrium for a porous domain in which water and CO₂ are segregated due to buoyancy effect. If capillary forces are considerable in the domain, the sharp interface between water and CO₂ in the macro scale will be replaced by a transition zone with a spectrum of saturations between phases (Figure 1.20). Due to the hydrostatic equilibrium, phase pressure at each depth can be related to the hydrostatic pressure of that phase:

$$P_w = \rho_w g z, \quad (1.15)$$

$$P_{CO_2} = \rho_{CO_2} g z. \quad (1.16)$$

Having the phase pressure, capillary pressure can be calculated by Equation 1.14. As capillary pressure is a function of wetting saturation, the phase saturations can be back-calculated from this functionality and the phase saturation distribution over the medium can be found (Figure 1.19):

$$S_w = P_c^{-1}(S_w). \quad (1.17)$$

We can derive mass and momentum balance for two-phase flow, similar to what we have seen for single-phase flow. The equations must be written for each phase. In Equation 1.4, the accumulation term must be considered only for one phase mass calculated by multiplying the total accumulation mass by phase saturation (S_α). Also the velocity is the phase velocity v_α , and the source/sink term must be written for the phase mass rate q_α .

For phase $\alpha = \{\text{water}, \text{CO}_2\}$, we have:

$$\int_{\Omega} \frac{\partial}{\partial t} (\phi \rho_\alpha S_\alpha) d\tau + \int_{\Gamma} (\rho_\alpha v_\alpha \cdot n) d\sigma = \int_{\Omega} q d\tau. \quad (1.18)$$

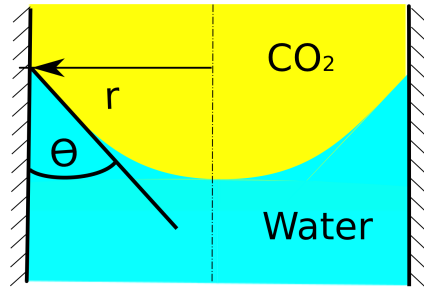


Figure 1.19: Capillary pressure distribution in the transition zone.

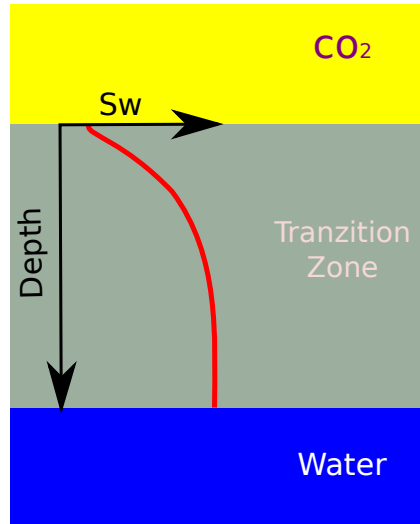


Figure 1.20: Saturation distribution in the capillary transition zone.

Darcy equation for two phases $\alpha = \{\text{water}, \text{CO}_2\}$ can be written in the following form:

$$v_\alpha = -\frac{K_{e\alpha}}{\mu_\alpha} \cdot (\nabla P_\alpha + \nabla D_\alpha). \quad (1.19)$$

Here, $K_{e\alpha}$ is the effective permeability for phase α and can be calculated from:

$$K_{e\alpha} = K_{abs} K_{r\alpha}, \quad (1.20)$$

where K_{abs} is the absolute rock permeability and $K_{r\alpha}$ is the relative permeability of phase α . P_α is the phase pressure and D_α is the gravity term for the phase specific gravity.

Similar to Equation 1.6, differential form of mass balance equation for each of phases $\alpha = \{\text{water}, \text{CO}_2\}$ is as follows:

$$\frac{\partial}{\partial t}(\phi \rho_\alpha S_\alpha) + \nabla \cdot (\rho_\alpha v_\alpha) = q_\alpha. \quad (1.21)$$

In this equation, q_α is the source/sink mass rate for phase α .

The phase saturations are related by the following equation:

$$S_{\text{water}} + S_{\text{co}_2} = 1. \quad (1.22)$$

Fluid properties change by pressure and temperature. Density is mainly a function of pressure and viscosity depends upon temperature. These functionalities, called by convention equation of state (EOS), must be coupled to the system to honor fluid attribute variability [20, 33].

Mass exchange between phases may happen leading to change in composition. That also influences the fluid properties. In the immiscible fluids, the mass exchange can be in small order leading to slight

changes in fluid properties. That can be modeled in a linear functionalities with respect to pressure and temperature.

Extensive mass exchange between phases results in more nonlinear fluid property variations that require a detailed equation of state. Also for highly miscible fluids and high mass transfer between phases, it might be better to write mass and momentum balance equations for components within phases in addition to phase equations.

There are number of approaches to formulate the primary unknowns in the system of flow equations. The direct way is to replace phase velocities from Equation 1.19 into Equation 1.21, leaving the phase pressures and water saturation as the primary unknowns. This ends in a set of strongly coupled equations.

A popular approach for formulating the set of flow equations is the fractional flow method [12]. In this method the total multiphase flow problem is treated as a single-phase flux of multi-phase mixture. Therefore, individual phases are described as a function of total flow. This leads to separate equations for pressure and saturation.

Pressure and saturation are defined for the total flow either global or pseudo globally and relate to the phase pressure and saturation with auxiliary equations. The fractional flow approach keeps the governing equations in the form of single flow equations, and numerical schemes for single-phase flow can be revised into efficient schemes for multi-phase problems.

Pressure and saturation equations have different mathematical nature: pressure has a diffusive character of an elliptical nature, which is numerically more stable than the saturation equation. Saturation equation is of convection-diffusion form with hyperbolic character in the convection part. The convection operator in saturation equation can be highly non-linear due to strong coupling of saturation and phase velocity. This nonlinearity can lead to shocks and discontinuities in the saturation solution.

As an example of fractional flow formulation, global pressure P_t is defined based on phase pressures:

$$P_t = \frac{1}{2}(P_w + P_{CO_2}) - \int_{S_w|P_c=0}^{S_w} (f_w - \frac{1}{2}) P'_c(S_w) dS_w, \quad (1.23)$$

where water fractional flow f_w is defined as:

$$f_w(S_w) = \frac{\frac{K_{rw}}{\mu_w}}{\frac{K_{rw}}{\mu_{CO_2}} + \frac{K_{rco_2}}{\mu_{CO_2}}}. \quad (1.24)$$

The total velocity is defined as:

$$v_t = v_w + v_{CO_2}. \quad (1.25)$$

If capillary and gravity effects are negligible, saturation equation can be solved analytically, e.g. via Buckley-Leverett technique, or method of characteristics.

1.7 Flow regimes

A major part of our studies includes modeling physical phenomena occurring within flow through porous media. Various phenomena occurs during a complete sequence of CO₂ sequestration. During injection the forces imposed by injector dominate the flow behavior in a region around the injector. When CO₂ plumes develop in a thin layer moving along the stratigraphical structure, a large interface between water and CO₂ enhances the diffusion phenomena and lets more CO₂ to be dissolved into water. Convection of water with dissolved CO₂ into the initial water in place leads to complicated flow regimes.

The injected CO₂ undergoes various stages until it is stored underground. We consider two stages in our studies: injection (and early migration), and long term migration. Many forces act on flow within medium, each of which requires a set of modeling parameters. Simplifying assumptions for flow modeling can be justified at each stage with relevance to dominating forces in the medium.

The following can be recognized as forces acting on the medium in the scale at which Darcy velocity is defined:

- Forces due to pressure gradient, mostly imposed by injectors (and/or producing wells)
- Gravity, due to buoyancy with density contrast between flowing phases. Gravity acts in the vertical direction.
- Capillary forces, due to interfacial tensions.
- Hysteresis, due to sequencing of imbibition and drainage during flow in the porous medium.
- Convection forces, due to gradient of density in one phase.
- Diffusion, due to concentration gradient of one component.
- Reaction, due to chemical reaction between phases and rock.

Modeling all forces acting on porous media is not practical, and we need to look at each flow regime separately by neglecting some forces that have a minor role. Herein, we discuss main forces during injection and within long term migration.

1.7.1 Injection and early migration

Injection of CO₂ in the underground happens by forcing CO₂ mass through injector into the medium. This pose a pressure gradient around the injector causing flow within the near bore region. Some authors call the force due to pressure difference ‘viscous force’, since viscosity has an important role in transferring the stress due to pressure difference in the porous medium resulting in fluid mobility. We use the same term throughout this thesis.

Viscous and gravity forces are the two major forces acting on the region around injector during injection. Depending on medium-fluid properties and distance from injection point, force balance changes. Gravity causes rapid phase separation resulting in upward movement of CO₂. Gravity forces dominate two-phase regions far from injector with lower viscous flow velocity compared to near well locations, where the flow velocity is high. At each place in the medium, a force balance results in a total force vector that may cause flow in a particular direction (Figure 1.21a).

Attempts in the literature on evaluating force interplay during a multiphase flow regime incorporating injection in the porous medium, employ sensitivity analysis on flow attribute such as flow velocity and pressure. Many authors try devising an analytical solution to the fairly simplified flow equations that are reduced by justified assumptions and are applicable to the problem [11, 16, 19, 26, 27, 57, 61, 71, 72]. Utilizing analytical solutions gives the flexibility of examining a wide range of parameter variations within the model, enjoying a fast evaluation of the corresponding flow behavior. Semi-analytical and numerical sensitivity analysis are also vastly performed in the literature to involve more physical modeling features in the flow performance evaluations[4, 5, 63].

The flow equations can be normalized to a dimensionless version that is used in many studies discussing the capillary and gravity influence on the flow. Herein, we give the method reported in [27]. If we assume an incompressible flow in one dimensional space for a location in domain Ω without any source/sink, Equation 1.21 reduces to the following for the wetting phase:

$$\phi \frac{\partial s_w}{\partial t} + \frac{\partial v_w}{\partial x} = 0, \quad (1.26)$$

in the x spatial dimension and Darcy equation for one dimension flow becomes:

$$v_w = -K \frac{k_{rw}}{\mu_w} \left(\frac{\partial P_w}{\partial t} + \rho_w g z \right). \quad (1.27)$$

Here, z is the elevation of flow and g is the gravitational acceleration. The system is closed by Equations 1.22 and 1.14. We can define the dimensionless variables as follows:

$$X^* = \frac{x}{L}; T^* = \frac{tv_t}{L\phi}; \text{ and } P_c^* = \frac{P_c}{\pi_c}, \quad (1.28)$$

where L is a length constant in the problem, and π_c is a capillary pressure normalizing constant. After reformulating Equation 1.26, fractional flow can be written in the following form:

$$f_w = G(S_w) + C(S_w) \frac{S_w}{X^*}, \quad (1.29)$$

where S_w is the normalized wetting phase saturation, G is the gravity contribution, and C is the capillary contribution to the flow. The gravity and capillary contributions, G and C , are expressed by quantities relative to the viscous force [35] and we have:

$$G(S_w) = F_w(1 - N_G k_{rw}), \quad (1.30)$$

$$C(S_w) = N_{nw} F_w k_{rw} \frac{dP_c}{dS_w}, \quad (1.31)$$

wherein:

$$F_w = \left(1 + \frac{k_{rw}}{\mu_{nw}} \frac{\mu_w}{k_{rw}}\right)^{-1}, \quad (1.32)$$

$$N_c = \frac{k\pi_c}{\mu_{nw} L v_t}, \quad (1.33)$$

$$N_G = \left(k \frac{(\rho_w - \rho_{nw}) g z}{\mu_{nw} v_t}\right). \quad (1.34)$$

Having these definitions, Equation 1.26 reshapes into:

$$\frac{\partial S_w}{\partial T^*} + \frac{dG(S_w)}{dS_w} \frac{\partial S_w}{\partial X^*} + \frac{\partial}{\partial X^*} \left(C(S_w) \frac{\partial S_w}{\partial X^*} \right) = 0. \quad (1.35)$$

Applying specific type of capillary pressure and relative permeability function may lead to simplified forms of Equation 1.35 with the possibility of having an analytical solution[72].

Some important conclusions in the literature from sensitivity studies on capillary, gravity and viscous forces are summarized here and inferred for CO₂ injection application:

- The gravity and capillary pressure will only influence the flow speed significantly for slow displacement rates. Therefor, around the injection point where normally fluids are flowing relatively with a high speed, the viscous forces are dominant.
- If capillary is of any significance, ignoring capillary forces in modeling the injection of CO₂ results in a pessimistic CO₂ sweep efficiency. Capillary helps in the spreading of CO₂ in the frontal CO₂-water interface.
- Less capillary forces in the porous medium, allows more space for CO₂. This in the macro scale enhances the density segregation due to gravity forces.

The main focus in the series of work in this thesis has been to assess the flow influence by heterogeneity during injection time and early CO₂ migration. For CO₂ injection problems, one objective is to maximize the rate of injection and aligned with that we use relatively high injection rates in our studies. Therefore, we did not include capillarity forces for modeling the high displacement rates within heterogeneities which can be justified by the results in the literature.

Table 1.1: Spatial scales for CO₂ storage. Ranges are extracted from [15].

Feature	Spatial scale
Capillary fringe	10cm->10m
Plume radius	10km->100km
Pressure perturbation	50km->500km
Migration distance	50km->500+km

Table 1.2: Temporal scales for CO₂ storage. Ranges are extracted from [15, 34].

Feature	Temporal scale
Density segregation	1 month->5+ years
Capillary segregation	1 year->50 years
Injection period	5 years->50 years
Convective mixing	20 years->1000 years
Plume migration	few hundred years->1000 years
Mineral reaction	500 years->100000 years

1.7.2 Long term migration

The injected CO₂ volume in the geological formation will travel below the sealing cap by buoyancy forces due to the density difference between water and CO₂. One concern is to have it stored safely, and the mobile CO₂ is at risk of leaking through any imperfections in the sealing layers and abandoned wells. Molecular diffusion occurs in the interface of water and CO₂ and this mass transfer from CO₂ plume into water increases the water density. Transition form of CO₂ from mobile phase into water with dissolved CO₂ is helping the safe storage of CO₂: the heavier water with dissolved CO₂ has the tendency of moving downward. Time scale for the convective mixing is of the order of several hundreds years (Table 1.2). Yet, this is not the end and the dissolved CO₂ can react with the porous medium ending up in a solid phase and it can be stored permanently in a process called mineral trapping. This is an extremely slow process and it can long to even hundreds of thousands of years [34].

Mixing of CO₂ and water in the long term happens through phases in different time scales and with various physical phenomena. Diffusion of CO₂ in water continues and the layer of water with dissolved CO₂ builds up below the CO₂ plume until it forms heavy parts convecting in the form of unstable fingers, as shown in Figure 1.21b.

The onset time for the convective mixing is important in terms of storage safety. This time depends on the Rayleigh number in the medium:

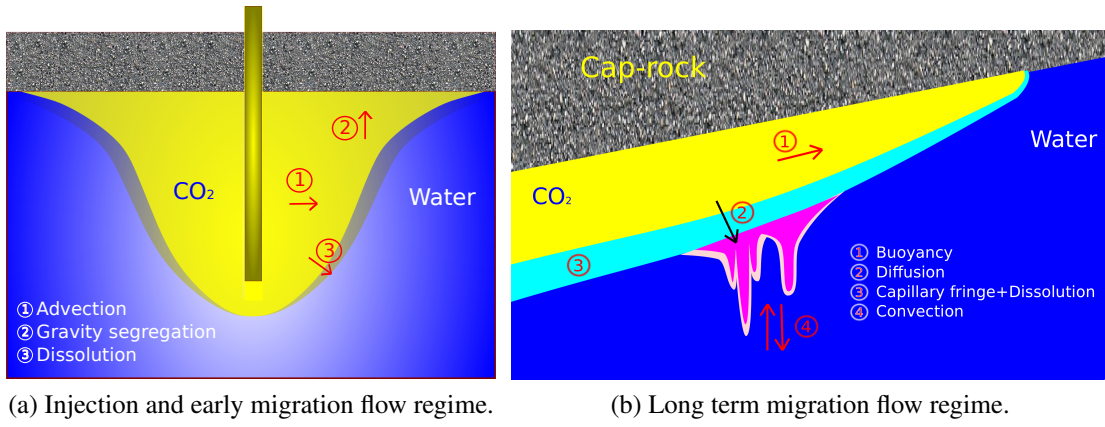
$$Ra = \frac{Kg\Delta\rho H}{D_c\phi\mu}. \quad (1.36)$$

Here, $\Delta\rho$ is the density difference between water and CO₂ phases and D_c is the diffusion coefficient of CO₂ into water phase. The higher density sitting on top of lower density makes an unstable system and the medium must have a minimum Rayleigh number in order to have a growing instability for a small perturbation in the medium. Heterogeneities in the medium can initiate perturbations, reducing the instability onset time [22, 36]. Therefore, heterogeneity is an important factor that must be considered when we are choosing an aquifer for CO₂ storage.

Capillary fringe in the plume can enhance the convective mixing onset. It can speed up the process up to five times [23].

The flow equations for convective mixing are a set of mass and momentum balance for component $c = \{\text{Water}, \text{CO}_2\}$ within phase $\alpha = \{\text{Wetting}, \text{Non-Wetting}\}$:

$$\frac{\partial}{\partial t} \sum_{\alpha} \phi S_{\alpha} \rho_{\alpha} X_{\alpha}^c + \nabla \cdot \sum_{\alpha} \rho_{\alpha} X_{\alpha}^c v_{\alpha} = 0, \quad (1.37)$$

Figure 1.21: Flow regimes in geological CO₂ storage.

and

$$v_\alpha = -\frac{k_{r\alpha} K}{\mu_\alpha} [\nabla P_\alpha - \rho_\alpha g z]. \quad (1.38)$$

where X_α^c is the mole fraction of component c in phase α [24].

1.8 Vertical averaging

In this section we discuss the common approach used in modeling the migration of CO₂ in large scale aquifers. This is a specific type of multi-scale modeling, at which we work with two models with two and three dimensions. A 2D model is extracted from the corresponding 3D model to reduce the computation costs and in some cases the accuracy can be enhanced by reducing the numerical diffusion as we will discuss here.

Spatial gradients of flux and pressure appear in the the flow equations can be decomposed into lateral and vertical components. For a three dimensional problem with the set of unit vectors $\{\vec{i}, \vec{j}, \vec{k}\}$, the gradient operator can be written as the following:

$$\nabla = \nabla_\ell + \nabla_v, \quad (1.39)$$

where:

$$\nabla = \frac{\partial}{\partial x} \vec{i} + \frac{\partial}{\partial y} \vec{j} + \frac{\partial}{\partial z} \vec{k}, \quad (1.40)$$

$$\nabla_\ell = \frac{\partial}{\partial x} \vec{i} + \frac{\partial}{\partial y} \vec{j}, \quad (1.41)$$

$$\nabla_v = \frac{\partial}{\partial z} \vec{k}. \quad (1.42)$$

x , y , and z are the location space components in the three directions.

The geological formation tops are not necessarily oriented horizontally, but they are normally close to horizontal. In CO₂ storage problems the lateral scale is orders of magnitude larger than the vertical direction. Therefore, the variations in the vertical direction are relatively negligible and for a quantity of interest Ψ we have:

$$\int_A \nabla \Psi d\tau \gg \int_\zeta \nabla \Psi dz, \quad (1.43)$$

where A is an arbitrary horizontal surface in the model and ζ is the vertical interval of the domain. Hence, with large lateral scales we can consider average values across the vertical direction for parameters and variables in the flow equations. This reduces the problem from 3D to 2D. In this case we

need to relate the parameters in the two dimensional and three dimensional problems. If this relation is not extremely non-linear the flow solutions can be obtained considerably faster on a two dimensional problem.

In a distance from the injection point, vertical equilibrium assumption is applicable. The density difference between water and CO₂ results in a rapid segregation of the two phases. A layer of CO₂ sits on top of water table and in the presence of considerable capillary forces a capillary transition zone forms between water and CO₂ zones (Figure 1.22).

The vertical equilibrium assumption facilitates the flow equation averaging across the vertical direction ζ . The phase distribution can be calculated from the volume calculations and capillary inverse function for the transition zone as mentioned in 1.6. Phase pressure variation versus depth follows the hydrostatic gravitational gradient for each phase.

The two dimensional version of flow equation can be written in the following form, assuming incompressible fluids [15, 53]:

$$\tilde{\phi} \frac{\partial \tilde{S}_\alpha}{\partial t} - \nabla_\ell \cdot \tilde{v}_\alpha = \tilde{\eta}_\alpha, \quad (1.44)$$

which follows by two dimensional Darcy equation:

$$\tilde{v}_\alpha = -\tilde{K} \tilde{\lambda}_\alpha (\nabla_\ell \tilde{P}_\alpha - \tilde{\rho}_\alpha \tilde{g}). \quad (1.45)$$

Herein, tilde sign denotes the two dimensional parameter or variable that is the vertically averaged of corresponding parameters and variables in the three dimensional problem. The averaging over vertical direction care defined in the following:

$$\tilde{\phi} = \frac{1}{H} \int_0^H \phi dz, \quad (1.46)$$

$$\tilde{K} = \frac{1}{H} \int_0^H K dz, \quad (1.47)$$

$$\tilde{\lambda}_\alpha = \frac{1}{H} K^{-1} \int_0^H K \lambda_\alpha dz. \quad (1.48)$$

Note that $\tilde{\lambda}_\alpha$ is a tensor, because it is defined such that the 2D Darcy equation is consistent with the 3D Darcy equation. The variables in the 2D equations are defined in the following:

$$\tilde{v}_\alpha = \frac{1}{H} \int_0^H v_\alpha dz, \quad (1.49)$$

$$\tilde{s}_\alpha = \frac{1}{\tilde{\phi} H} \int_0^H \phi s_\alpha dz, \quad (1.50)$$

$$\tilde{P}_\alpha = p_\alpha(z_D), \quad (1.51)$$

$$\tilde{\eta}_\alpha = \frac{1}{H} \int_0^H \eta_\alpha dz. \quad (1.52)$$

The hydrostatic equilibrium results in a constant phase pressure gradient over the vertical direction. Therefor, the phase pressure at any datum depth z_D in the medium can be used into the 2D flow equations.

Accuracy of vertical averaging approach within CO₂ storage context has been examined in many works in the literature [17, 32, 45, 53]. It has been shown that vertical averaging is applicable to large scale CO₂ studies. The numerical aspects and speed up of the method compared to three dimensional problem are studied in [32, 46], where a second order speedup is reported. Lie et al. [45] have shown the influence of vertical discretization in the three dimensional models which can fail in low resolutions to capture the thin layer of CO₂ plume migrating beneath the top sealing surface in the formation. The vertical averaging approach can handle this issue by considering the water and CO₂ interface in

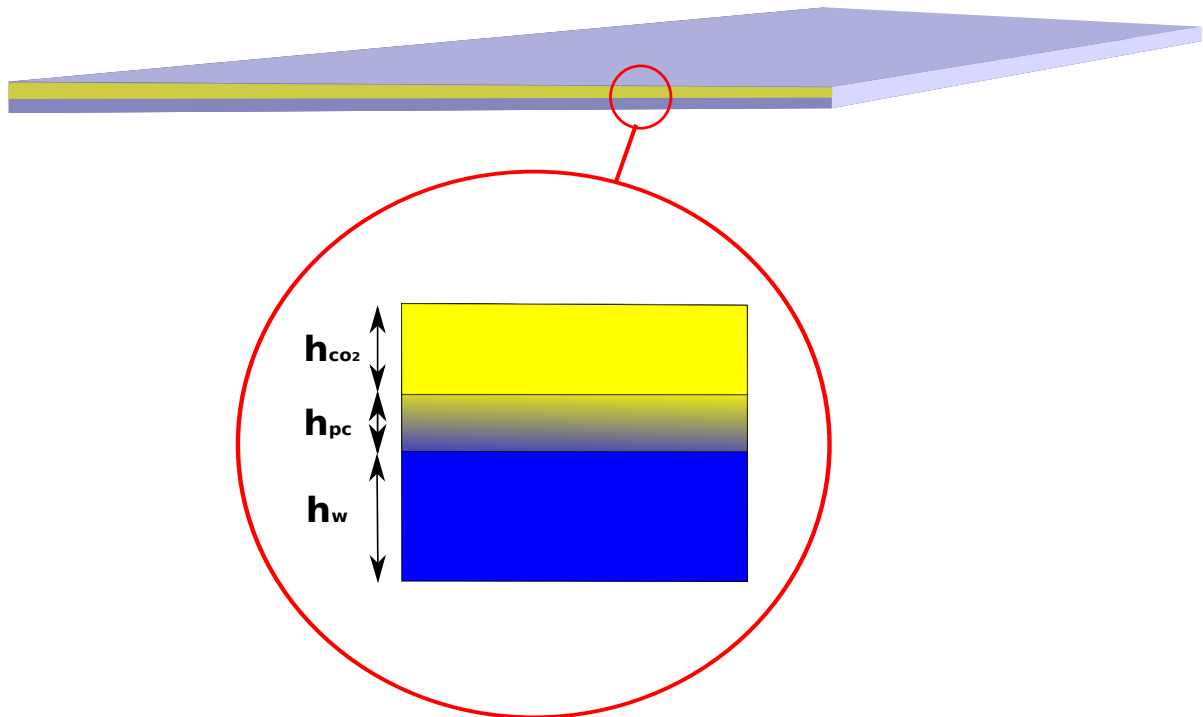


Figure 1.22: Hydrostatic equilibrium condition results in three zones: the CO_2 zone with thickness $h_{\text{co}2}$, the water table with thickness h_w , and the capillary transition zone h_{pc} .

calculating the vertically averaged parameters in the model. A comparison between three and two dimensional models has been done on various aspects in [53].

The influence of topography in modeling the CO_2 migration and estimating the storage fate has been shown in [32, 67] by examining different geometries and heterogeneities in the domain. These conclusions suggest that the significance of the model top surface is more than the small order flow in the model vertical thickness.

The studies reported in this thesis concern the flow near injector and early times of plume development. Therefore vertical equilibrium would benefit larger scales with big portion of model in vertical equilibrium. We do our flow modeling by including the three dimensions and for the quantitative uncertainty analysis we employ a polynomial approximation (Section 1.10).

1.9 Flow modeling

We use a standard porous media simulator to solve the flow equations in the medium. The solution is based on finite difference method and the following assumptions are taken:

- Two compressible phases are considered in the medium: water and super critical CO_2 .
- No mass exchange occurs between the two considered phases.
- No heat exchange is considered.

1.9.1 Numerical scheme

The employed simulator uses two-point finite difference scheme to solve Equation 1.21 on a Cartesian grid. The Darcy equation for two-phases can be written in a difference. This makes the flow equation into cell a from the neighboring cell b:

$$F_{ab\alpha} = T_{ab} M_{a\alpha} \Delta \psi_\alpha. \quad (1.53)$$

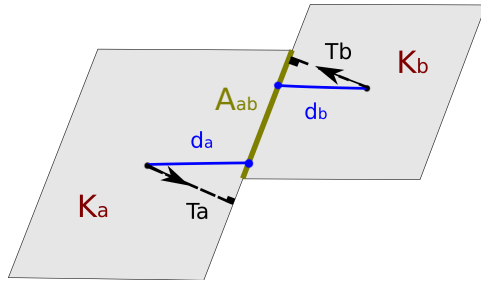


Figure 1.23: Transmissibility calculation for two cells a and b.

Here, T_{ab} is the transmissibility of medium between the two cells. $M_{a\alpha}$ is the mobility of phase α that is taken upstream of the flow from cell a, and $\Delta\psi_\alpha$ is the pressure and gravity term difference between two cell centers.

Transmissibility for two neighboring cells (i.e., sharing a face area, see Figure 1.23) is calculated by harmonic average of transmissibilities from the center of each cell to the center of the cells mutual face within that cell:

$$T_{ab} = \frac{1}{\frac{1}{T_a} + \frac{1}{T_b}}. \quad (1.54)$$

Each half transmissibility is calculated by an inner product between the permeability of the cell K_a , the mutual area between cells A_{ab} , and the distance from cell center to the mutual face center d_a :

$$T_a = K_a \cdot d_a \cdot A_{ab}. \quad (1.55)$$

Mobility term in Equation 1.53 is defined as follows:

$$M_{a\alpha} = \frac{k_{r\alpha}}{B_\alpha \mu_\alpha}, \quad (1.56)$$

where $k_{r\alpha}$ is the relative permeability of phase α , μ_α is the viscosity of phase α , and B_α is the formation volume factor of phase α which is defined as :

$$B_\alpha = \frac{\text{Volume at surface condition}}{\text{Volume at formation condition}} = \frac{V_{s\alpha}}{V_{r\alpha}}. \quad (1.57)$$

Formation volume factor definition is connected to compressibility of the fluid to change volume at surface and in the geological formation condition, but it is defined in this way in the simulator to honor cases where a fluid like oil loses its dissolved gas while being produced at surface pressure. Since we assume no mass exchange between phases in our study, here the formation volume factor works like compressibility of the fluid. Formation volume factor is a function of pressure.

Slight compressibility is considered for phases in our study, and phase density is defined as a function of pressure:

$$\rho_\alpha(P) = \frac{\rho_{0\alpha}}{B_\alpha(P)}. \quad (1.58)$$

Here, $\rho_{0\alpha}$ is the density of phase α at surface condition.

Wells are defined as source or sink in Equation 1.21. In reality wells are a void space drilled in the porous medium and the flow into the well-bore and up to surface for production wells (and vice-versa for injectors) goes through a pressure change that must be modeled separately from the porous medium.

Figure 1.24 shows a schematic pressure distribution around the injector. The well radius is much smaller than the simulation cell containing the well and the pressure in the bottom-hole is different than the cell pressure. The well bottom-hole pressure can be related to the cell pressure containing the well by a separate approximation that can be coupled with the flow equations in the grid model. Flow equation for phase α between the cell center and the well for an injector is written as follows:

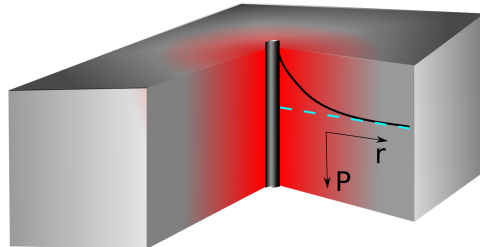


Figure 1.24: Well modeling inside a simulation cell.

$$\eta_\alpha = T_w \cdot M_\alpha \cdot [P_w - P_1]. \quad (1.59)$$

η_α is the volumetric injection rate of phase α , P_w is the injector bottom-hole pressure, P_1 is the cell pressure, T_w is the transmissibility between the cell and the injection well-bore, and M_α is the mobility of injection flow into the cell.

A region can be assumed by a radius r_e at which the pressure is equal to the cell pressure. Approximating the flow near the well-bore by Equation 1.12, the transmissibility for this region can be found from the analytical solution to Equation 1.12:

$$T_w = \frac{cK \cdot h}{\ln(\frac{r_e}{r_w})}, \quad (1.60)$$

where c is a unit conversion constant, h is the medium thickness, K is the medium rock permeability, and r_w is the well radius. Here, we assume that the well is completed and connected in the entire thickness of the cell h and there is no skin effect in the well. The Equation 1.60 can be extended to model wells with partial completions and skins. r_e in Equation 1.60 is estimated from Peaceman formula and can be related to the cell geometry:

$$r_e = 0.28 \frac{\left[\delta_x^2 \left(\frac{K_y}{K_x} \right)^{\frac{1}{2}} + \delta_y^2 \left(\frac{K_x}{K_y} \right)^{\frac{1}{2}} \right]^{\frac{1}{2}}}{\left(\frac{K_y}{K_x} \right)^{\frac{1}{4}} + \left(\frac{K_x}{K_y} \right)^{\frac{1}{4}}}. \quad (1.61)$$

Here, K_x and K_y are the permeabilities in X and Y directions and δ_x and δ_y are the cell sizes in these directions. This equation assumes a vertical well and a diagonal permeability tensor. It can be modified for more general cases.

1.9.2 Flow scenarios

All of the realizations have dimensions of $3 \text{ km} \times 9 \text{ km} \times 80 \text{ m}$, which is enough to capture variations in the designed geological features. While the volume of the realizations is large enough to capture major parts of the injected volume, the pressure disturbance imposed by the injector can go beyond this scale. To compensate for the size, we choose hydrostatics boundary conditions for the models. The open boundaries are modeled by considering a huge pore volume for the outer cells in the model that represent the boundary. Figure 1.25 shows the boundary condition defined in the model.

We consider the injection of 20% of the total model pore volume, which amounts to 40 MM m^3 . This volume is injected into realizations in three different scenarios. In the first scenario, the injection is forced to finish in 30 years and the pressure in the system is allowed to rise unlimitedly. Linear relative permeability functions are considered in this scenario. The purpose of the first scenario is to examine the flow distribution in the medium influenced by geological heterogeneity. Linear assumption for relative permeabilities is taken to speed up the flow within the medium. The relative permeability curvature has shown a significant influence on the pressure behavior in the aquifer.

In the second scenario, the injector operates with the same fixed rate as in the first scenario and the relative permeability curves are chosen to be quadratic functions. Quadratic relative permeability curves

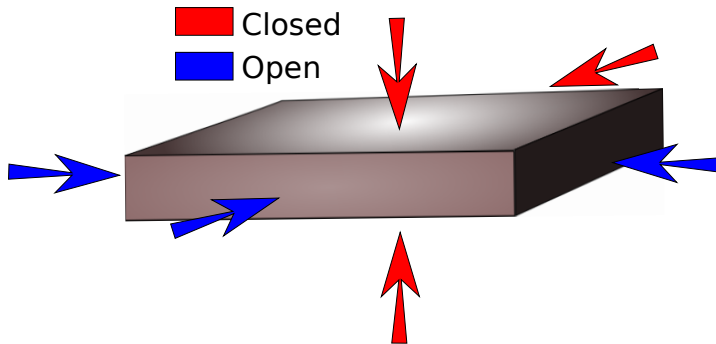


Figure 1.25: Top, bottom, and upper side boundaries are closed and the rest are open to the flow.

cause lower flow mobility in the medium compared to the linear function, and by forcing the injector with a fixed volumetric rate of injection, the pressure rises significantly in the aquifer. This leads us to the third injection scenario, where the injector is controlled by pressure rather than volumetric rate. Thus, injection time is variable depending on the injectivity of the medium.

Only one injector is considered in the study. With one injector, it is easier to study the flow behavior and the plume development within the medium. The injector is located in the flank and to increase the sweep efficiency for the up-moving CO₂ plume, the injector is completed only in the lower part of the aquifer. The injector location and the completed layers are fixed for all of the realizations. The studies here aim to identify the influence of uncertainty on injectivity and fixing a place for injection helps in achieving this goal. In a deterministic case, we can complete the well in the best quality layers.

There are few locations of distorted geometries in the faulted realizations that may be considered as structural traps for the injected CO₂. The topography in the SAIGUP realizations is simple and does not cover the variational space to be used in a sensitivity analysis. The slight inclination in the structural geometry of the medium, from the flank up to the crest, leads the injected CO₂ to accumulate in the crest and below the faulted side of the aquifer. The structural trapping due to variational morphology is studied in IGEMS, which is a sister project to MatMora (for example, see [67]).

In a homogeneous medium, we expect the CO₂ to accumulate under the cap-rock. A small fraction of the injected CO₂ will escape through the open boundary near the injection well and the rest of it will stay within the medium in two forms that we refer to as mobile and residual volumes. As the CO₂ moves through the rock, part of it stays in the smaller pores by capillary trapping process and can not be discharged by brine. The other parts move through the larger pores and can be displaced by water in an imbibition process. This volume is called mobile. As we are interested in storing the CO₂ permanently and safely, increasing the trapped volume is in line with the objective of minimizing the leakage risk and maximizing the storage capacity. Likewise, the more mobile volume of CO₂ exists in the medium, the more will be the risk of leakage.

Defining the boundary condition of the aquifer of interest can influence the flow behavior in the system. One advantage of aquifers for carbon storage is the availability of large aquifers to provide the required accommodation space. Computational costs make that more feasible to model the flow locally and in the part of the aquifer that is going through more pronounced changes in flow behavior. Therefor, we can choose the boundaries of the model inside the aquifer in a volume that is containing the injection wells and the areas effected by them. Hydrostatic open boundary condition is a choice for the system boundaries to include the aquifer parts that fall outside the boundaries (Fig. 1.26).

The underground network of aquifer systems can be connected via geological channeling and conductive features. Some aquifers might be active and connected to the surface and expand in volume by variations in water influx due to seasonal rains. This can impose an external force on the system boundaries considered in a storage problem. Fig. 1.26 shows the water influx through the boundaries of the system due to external aquifer activities. We consider the external support by imposing a higher pressure than the hydrostatic pressure on the boundary of the model.

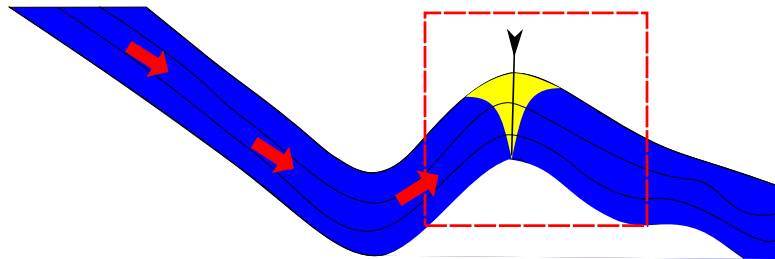


Figure 1.26: External pressure drive.

1.9.3 Flow responses

The primary unknowns in the flow model are the CO₂ pressure and the saturation distribution at different times. From the simulation output, we can derive quantities that address the feasibility of CO₂ injection, these quantities include a number of flow responses related to the CO₂ injection and migration problems. Each of these responses are directly or indirectly a measure of success for the operation within a specific realization. In the following, we give a brief description of each of them:

Boundary fluxes: The flux out of open boundaries is a measure of sweep efficiency for the CO₂ plume. Channeling can lead to early CO₂ breakthrough at boundaries and we prefer cases with less out-fluxes through open boundaries. The out-flux through the down open boundary, which is closer to the injector, is a potential loss for the injected volume. After the injection stops, some of the CO₂ that has left the domain comes in again due to gravity segregation effect.

Total mobile and residual CO₂ volume: If the CO₂ saturation is below the critical value, it will be immobile in the bulk flow, although not in the molecular sense. Less mobile CO₂ means less risk of leakage and more residual volumes (with saturations less than the critical) resulting from a more efficient volume sweep as preferable. We use critical saturation of 0.2 for both water and CO₂. During injection time the flow process is mainly drainage but after injection imbibition also happens and increases the residual trapped CO₂.

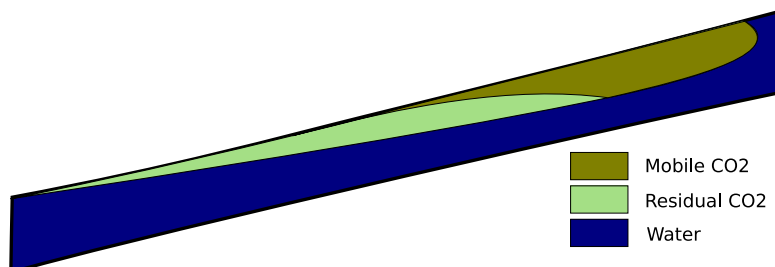


Figure 1.27: Mobile and residual CO₂ volume.

Total number of CO₂ plumes and largest plume: To estimate the risk of leakage from the cap-rock, we assume that all mobile CO₂ connected to a leakage point will escape out of the reservoir. Hence, it is preferable if the total mobile CO₂ volume is split into smaller plumes rather than forming a big mobile plume. Though the area exposed to potential leakage points will increase by splitting the plume, yet the volume reduction is overtaking the area effect. We looked at the largest plume size, the number of plumes, and other statistical parameters.

Average aquifer pressure: Average aquifer pressure is one of the most important responses to be considered. The pressure response in general shows a sharp jump at the start of injection and a declining trend during the injection and plume migration.

As soon as the injection starts, a pulse of pressure goes through the medium, introducing a pressure buildup in the aquifer. When the pressure wave reaches the open boundary, the aquifer pressure starts declining to a level maintained by the injector. When the injector stops operation, the pressure support will be removed and the pressure drops and declines until it reaches equilibrium.

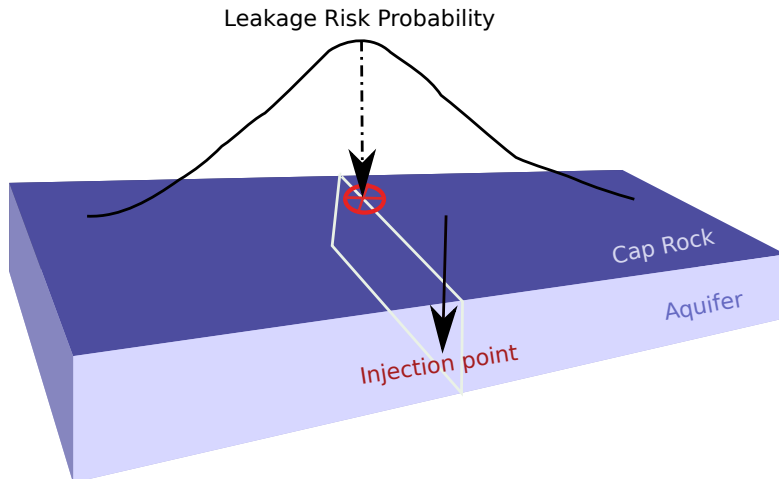


Figure 1.28: We use a 2D Gaussian distribution for leakage probability on the cap-rock.

Leakage risk: During injection operation the foremost important issue is the aquifer pressure which as discussed earlier may lead to fractures in the cap-rock. On the other hand, the cap-rock break depends on lithology and sealing thickness and differs from point to point. Some weaker locations can be the most probable to break and start leaking if any mobile CO₂ exists there.

Geo-mechanical modeling of aquifer combined with flow modeling in the medium are very costly to be used in uncertainty assessment processes. To avoid expensive computations, the idea in this thesis is to model the possible breakings on the cap-rock (considering the stress stream in the medium) by introducing a probability measure on the cap-rock. This measure can be used to evaluate different cases for their risk of leakage, considering the CO₂ distribution under the cap-rock.

Here, we define the probability of leakage as a measure on the cap-rock that assigns a value to each point of the cap-rock, modeling the relative weakness of the cap-rock and the medium at that point. If for example both the cap-rock and the aquifer are continuous homogeneous layers with constant thickness, then the point of cap-rock that sits on the highest point of the injection slice can be the most probable place for leakage in case of dramatic pressure increase in the well: the stress stream is more in the injection slice and the CO₂ accumulation occurs on the topmost part of the mentioned slice. Then one may consider a 2D-Gaussian probability distribution on the cap-rock, centered above the injection slice.

If the medium is heterogeneous or tilted, the injected CO₂ may be distributed in different number and sizes of plumes below the cap-rock. Therefore, in addition to the probability of breaking for each point of cap-rock, one must consider the CO₂ connected volume that is attached to that point.

Since we have neither the cap-rock model nor the geo-mechanical properties of the SAIGUP models, we use a simple 2D-Gaussian leakage probability distribution centered at a point on the crest which is in the same slice as the injection point (Fig. 1.28). We calculate the probability of each cell in the top layer and using the simulation results for the case, we weight it by the CO₂ saturation of that cell and the plume size that the cell is attached to. Summing up the values of the topmost cells, we assign a single number to the case which we call leakage risk of the case. One may weight the case risk value with the average pressure in the system, such that higher pressure gives a bigger weight.

One way to report the described responses and their relations to the uncertain parameters in one graph is to use scatter plots. Each case will then be represented by a marker sign with attributes dedicated to the set of geological parameter levels used in that case. Figure 1.29 shows some of the codes used in the study. That will be used later in the thesis in the papers reporting from our study.

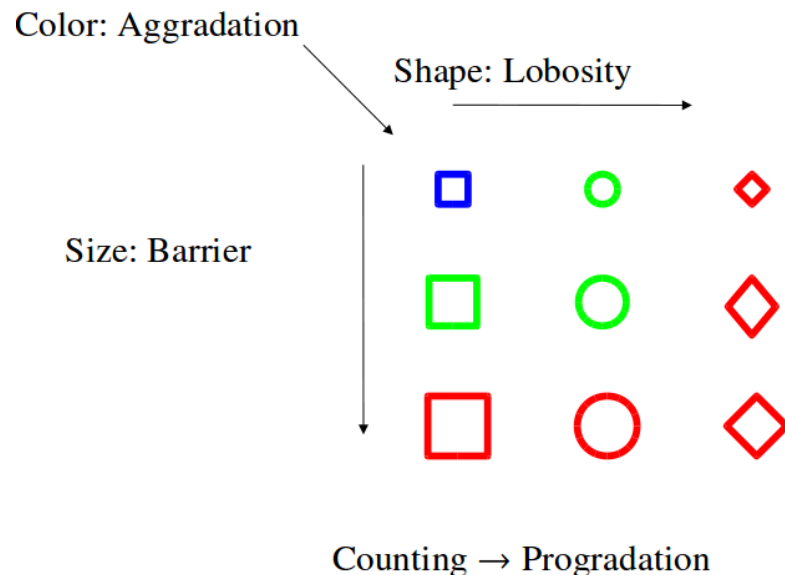


Figure 1.29: Marker codes used to plot the simulation results of all cases together.

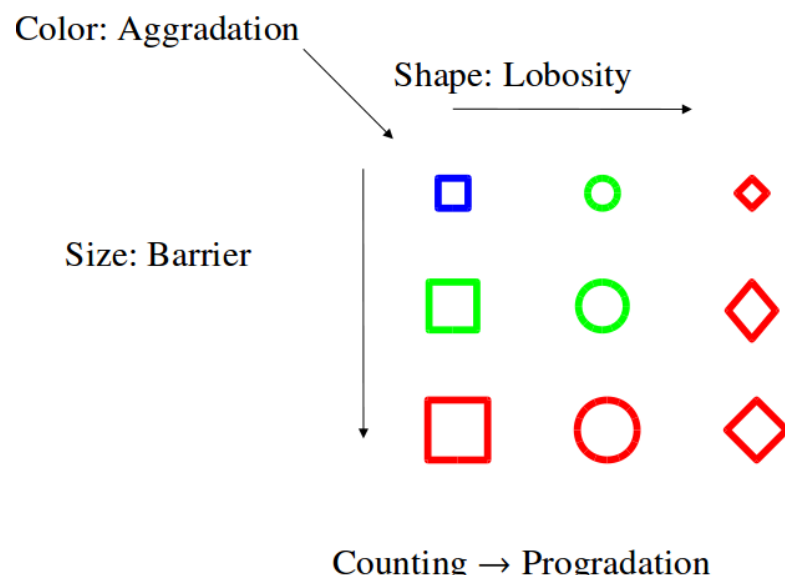
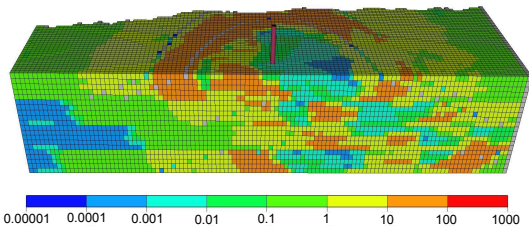
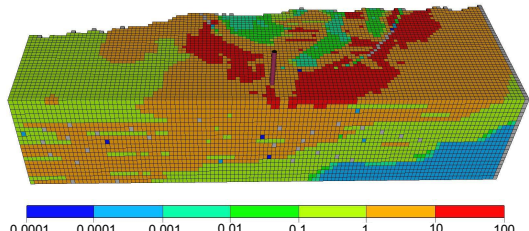


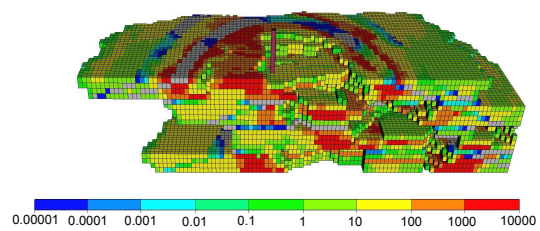
Figure 1.30: Marker codes used to plot the simulation results of all cases together.



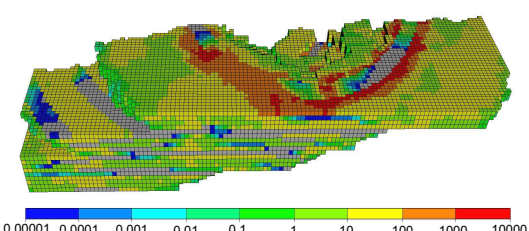
(a)



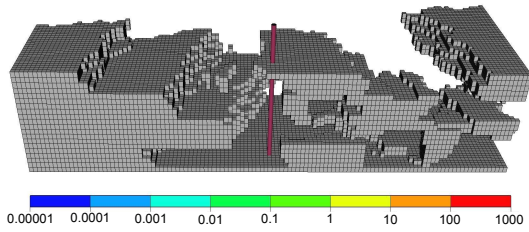
(b)



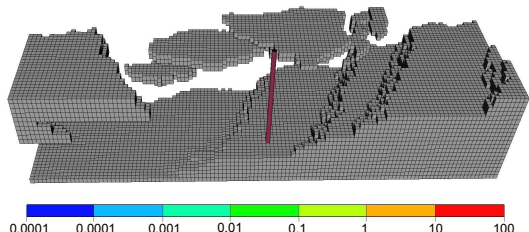
(c)



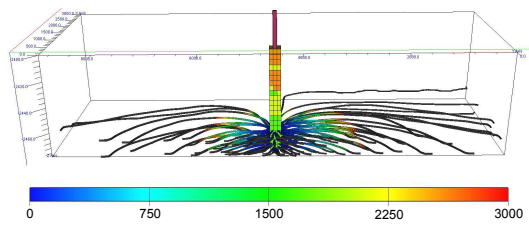
(d)



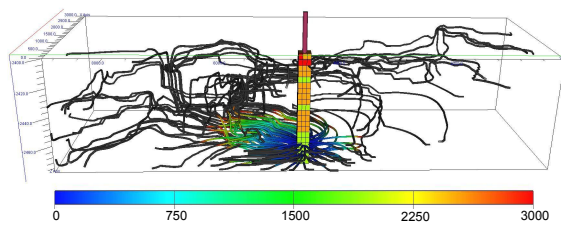
(e)



(f)



(g)



(h)

1.10 Sensitivity and risk analysis

Mathematical models developed to approximate the injected CO₂ in the storage sites consist of several steps, including the determination of parameters which are the most influential on the model outputs. Sensitivity analysis can serve as a guide to any further use of the model.

In the initial sensitivity analysis performed on geological uncertain parameters of our studies, we use the large number of detailed flow simulations and measure the variability of model responses with respect to each level of the uncertain parameters.

We can obtain histograms of response Γ for three different levels of parameter α (i.e., low, medium, and high) by performing simulations over all geological realizations. Measuring the mean response value on each histogram results in an average for all cases with a fixed level for parameter α . Having three average points for low, medium, and high levels of parameter α , a line can be fitted to those points that approximates the trend of variations of response Γ versus the increase in levels of para α .

Assuming an equal probability for each level, the model output variations are examined by looking at each response at two important simulation times, i.e., end of injection and end of simulation. In order to study the input variations over a higher resolution, demands for a fast flow modeler. We use a response surface method that is explained in the next section in details.

1.10.1 Stochastic analysis

Complicated physical phenomenon must be modeled as a stochastic process. Uncertainty reduction in different part of modeling requires a better understanding and description of input parameters and dependency rules within the system. Parameters can be ranked in the order of their influence on the model output. Knowing the most influential parameters helps in treating the stochastic nature of the process.

Sensitivity analysis serves in identification and evaluation of important model parameters. The European commissions and the United States environment protection agency recommend using sensitivity analysis in the context of extended compact assessment for uncertainty reduction strategies and policy making [65].

As discussed in the earlier sections, various sources of uncertainties are embedded within CO₂ storage modeling and operations. The devotion of our research has been on geological uncertainty and its consequences. The procedure used here to identify the relative importance of uncertain geological parameters via sensitivity analysis and the corresponding risk assessment is a general work-flow that can be applied to any type of uncertainties in the model inputs.

Our research continues by employing a stochastic response surface method that approximates the flow responses by projecting them on high-dimensional polynomials. In particular, we use arbitrary polynomial chaos (aPC) expansions, which consists of orthogonal polynomial bases that are constructed according to the uncertainties in the input parameters. The approach is flexible with respect to the quantification of probabilities for uncertain parameters and can be applied in studies with limited knowledge of probabilities.

The reduced model approximated by aPC is considerably faster than the original detailed one, and thus it provides a promising start point for global sensitivity analysis and probabilistic risk assessment. Variance based global sensitivity analysis methods have shown success in non-linear and complex problems[62].

The system can be decomposed into approximating functions of input parameters, and this makes it easy to implement methods based on variance. The bottle-neck of variance-based approaches can be their computational costs. In our case, the variance in output responses can be set equal to the variance of polynomial components calculated for each input parameters. Polynomials are relatively very fast and this makes it efficient to implement a variance based sensitivity analysis. Furthermore, the fact that the response surface has known polynomial properties simplifies the approach significantly. Finally, the speed of polynomial approximation makes it feasible to perform an intensive probabilistic

risk assessment via Monte-Carlo process over high resolution input variation.

1.10.2 Arbitrary polynomial chaos expansion

Statistical accuracy of a Monte-Carlo process is highly sensitive to the resolution of variational inputs. A response surface method assisting a Monte-Carlo procedure must be constructed on a dense Cartesian grid, which will be computationally demanding. We explore an alternative method which only requires a minimum number of model evaluations to construct the approximating response surface. The approach we use is based on the aPC as described in [58]. The main idea is to construct the approximating response surface by projecting the response on orthogonal polynomial bases within uncertain parameter space. Therefore, uncertainty of input parameters is involved in the process from the initial steps of the work-flow. This approach is an advanced statistical regress on method that offers an efficient and accurate way of including non- l near effects in stochastic analysis, see e.g., [25, 29, 73]. The method is examined for accuracy and one attractive feature of PCE is the high-order approximation of error propagation as well as its computational speed [59] when compared to Monte-Carlo processes.

Earlier PCE techniques put the restriction of specified types of uncertainty distribution functions to be used in the work-flow. In contrast, the arbitrary polynomial chaos (aPC) is flexible to accommodate for a wide range of data distribution [58]. The aPC can work even in cases with limited uncertainty information reduced in a few statistical moments of samples. They can be specified either analytically (as probability density, cumulative distribution functions), numerically as histograms, or as raw data sets. In terms of performance, the aPC approach shows an improved convergence applied to input distribution that fall outside the range of classical PCE.

In general, an approximation of system response Γ , can be written as a functionality of uncertain input parameters Θ :

$$\Gamma \approx \Upsilon(\Theta). \quad (1.62)$$

Uncertainty of input parameters Θ can be represented by mapping h from random variable space xi to random input space Θ

$$\Theta = h(\xi). \quad (1.63)$$

As discussed earlier, h can be an analytical or numerical representation. Approximation 1.62 can be expressed in the parametric mathematical form. We use a polynomial expression to approximate the flow responses. This polynomial consists of coefficients that do not necessarily have a direct physical interpretation. Instead, we must define these coefficient such that the prediction by our polynomial functional matches some available realistic responses. These responses must be obtained either from real data measurements or via detailed flow modeling tools. This type of approximation is data-driven and we can rewrite approximation in 1.62 as follows:

$$\Gamma \approx \Upsilon(\Theta) = v(\Theta, \alpha). \quad (1.64)$$

In this relation, Θ is the input parameters and α is in the data driven parameter space, which represents the dependency between input and output of the system. First, we specify α . Then given Θ , the responses Γ can be estimated. In many practical problems, input parameters are expressed in terms of random variables and a functional form is defined to quantify the system responses. This functional expression can be in different forms, from simple linear mapping to very complicated non-linear forms.

The aPC approach involves the uncertainty of input parameters in constructing the polynomial bases. The responses of the system can be expanded into the space of these bases. This expression is specified by constant coefficient c_i :

$$\Gamma \approx \sum_{i=1}^{n_c} c_i \Pi_i(\Theta). \quad (1.65)$$

Here, n_c is the number of expansion terms, c_i are the expansion coefficients, and Π_i are the multi-dimensional polynomials for the variables Θ , $\Theta = [\theta_1, \dots, \theta_n]$. The number n_c of unknown coefficients

c_i depends on the degree d of the approximating polynomial, and the number of considered parameters n :

$$n_c = \frac{(d+n)!}{d! \times n!}. \quad (1.66)$$

Polynomials Π_i in the Expansion 1.65 consist of polynomial bases P_l , with l ranging from zero up to the approximation degree d . These bases are orthogonal, i.e., every pair of non-identical bases fulfill the following condition:

$$\int_{I \in \Omega} \omega P_l P_m d\tau(\Theta) = \delta_{lm}, \quad (1.67)$$

where ω is a weight function, δ is the Kronecker delta function, and τ is the measure for input variable space. We choose the weight to be one, i.e., $\omega := 1$.

According to [58], the orthogonal polynomial basis satisfying Equation (1.67) can be obtained from the solution of the following linear system of equations:

$$\begin{bmatrix} \mu_0 & \mu_1 & \dots & \mu_k \\ \mu_1 & \mu_2 & \dots & \mu_{k+1} \\ \dots & \dots & \dots & \dots \\ \mu_{k-1} & \mu_k & \dots & \mu_{2k-1} \\ 0 & 0 & \dots & 1 \end{bmatrix} \begin{bmatrix} P_0^{(k)} \\ P_1^{(k)} \\ \dots \\ P_{k-1}^{(k)} \\ P_k^{(k)} \end{bmatrix} = \begin{bmatrix} 0 \\ 0 \\ \dots \\ 0 \\ 1 \end{bmatrix}, \quad (1.68)$$

Here, μ_k is the k^{th} non-central (raw) statistical moment of random input variable, which is defined as:

$$\mu_k = \int_{\Theta \in \Omega} \Theta^k d\tau(\Theta). \quad (1.69)$$

Thus, arbitrary polynomial chaos expansion base on Equation 1.68 only demands the existence of a finite number of moments, and does not require the exact knowledge or even existence of probability density functions. An interesting aspect is that only moments up to twice the order of expansion matter. This means, that there is no need for any kind of assumptions for data probability distribution leading to subjectivity artifacts as discussed earlier.

The PCE techniques are divided into intrusive [31, 50, 70] and non-intrusive [40, 42, 43, 59] approaches. Intrusive techniques require modifications in the system of governing equations. In some cases, this can end up in semi-analytical methods that are used for simpler stochastic analysis studies (e.g., stochastic Galerkin method). However, the intrusive approaches can be very complex and analytically cumbersome and can not be implemented for industrial applications. In contrast to intrusive techniques, the non-intrusive methods are vastly used in practical studies. These methods do not require any symbolic manipulations of the governing equations. The sparse quadrature and the probabilistic collocation method (PCM, [43, 59]) are among the non-intrusive technique. In a simple sense, PCM can be considered as a mathematically optimized interpolation of model output for various parameter sets. The polynomial interpolation is based on minimal model evaluations in optimally chosen set of parameters that are called collocation points. Hence, the challenge in these techniques is to find a balance between accuracy and speed to evaluate the uncertainty in the physical processes.

The collocation formulation has the advantage of treating the model as a black-box. This formulation requires the corresponding output to be known in the collocation set of input parameters obtained from any acceptable mapping between input and output in the system.

According to [69], the optimal choice of collocation points corresponds to the roots of the polynomial of one degree higher ($d + 1$) than the order used in the chaos expansion (d). This strategy is based on the theory of Gaussian integration (e.g., [3]).

For multi-parameter analysis, the full tensor grid of available points from the original integration rule is $(d + 1)^n$, which is larger than the necessary number M of collocation points. This might be used for low-order ($1^{\text{st}}, 2^{\text{nd}}$) analysis of limited number of parameters. However, for large number of parameters and high order of polynomial approximations, the full grid becomes computationally

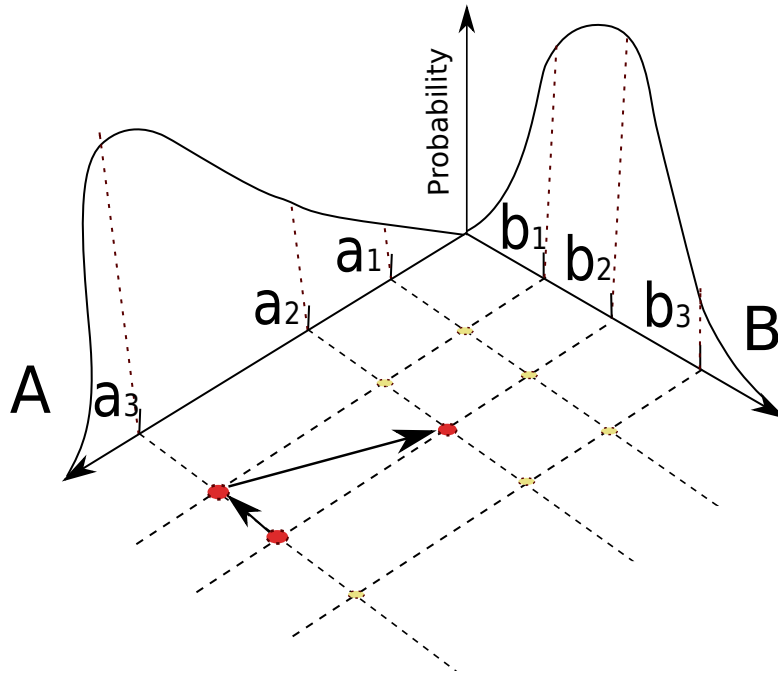


Figure 1.31: Collocation points are combined in different uncertainty directions such that the total probability in all directions is maximized.

cumbersome. In the collocation approach, minimal tensor of grid point set is chosen that is a scarce set of collocation points that are chosen from the most probable regions based on the parameter probability distributions (See [43, 58, 59]). This way the modeler can extract a lot of information in the main range of the parameter distribution (Figure 1.31).

We implement the probabilistic collocation method for computing the coefficients c_i in Equation 1.65. The weighted-residual method in the random space is defined as [43]:

$$\int \left[\Gamma - \sum_{i=1}^{n_c} c_i \Pi_i(\Theta) \right] w(\Theta) p(\Theta) d\tau = 0, \quad (1.70)$$

where $w(\Theta)$ is the weighting function and $p(\Theta)$ is the joint probability density function of Θ . By substituting the weight function in Equation 1.70 with Delta function, the equation reduces to

$$\Gamma_c - \sum_{i=1}^{n_c} c_i \Pi_i(\Theta_c) = 0. \quad (1.71)$$

In this equation, Γ_c and Θ_c are the responses and input parameters in the collocation points. Having the Θ_c chosen based on the probability distributions of input parameters, and Γ_c from the minimal model evaluations on Θ_c , we can solve Equation 1.71 and find the coefficients c_i .

1.10.3 Sensitivity analysis

Sensitivity analysis helps in understanding the degree of dependency of system responses to the input parameters. When the input parameters are uncertain in value, the model predictions will consist of uncertainties that must be eliminated for a robust and precise prediction. Therefore, sensitivity analysis can be useful both in optimizing the system performance and in studying the variation in performance coming from the stochastic nature of the system.

Global sensitivity analysis covers the entire variational space for uncertain parameters, while other methods, like the gradient-based methods, are limited in the scope influence of the parameters.

Variance-based methods are very popular among different types of sensitivity analysis methods. Variance-based methods provide global sensitivity and work for general non-linear problems. When the response is decomposed into simpler components (for instance, polynomial bases), it is easier to decompose the unconditional variance in the output into terms due to individual parameters and the interaction between them. It is possible then to rank the input parameters based on their contribution to the output variance [62, 66].

Following the linear sensitivity analysis performed initially in the study on the extensive detailed simulations, we tackle the global sensitivity analysis based on the aPC technique. This approach is well described in [58, 60]. Morris method [54] considers a uniform importance of input parameters within predefined intervals. We use a weighted global sensitivity in a more flexible approach accounting for arbitrary bounds and parameters with different importance defined by weighting functions. The big advantage of aPC-based sensitivity methods is their low computational costs for obtaining global sensitivity analysis. The aPC based-method places the parameter sets for model evaluation at an optimized spacing in parameter space. This can be interpreted as fitting polynomials to the model response. These polynomials approximate the model over the entire parameter space in a weighted least-square sense. This is more beneficial to computing a tangent or local second derivatives (compare FORM, SORM methods, e.g., [41]) that approximate the model well just around one point in the parameter space.

As an advantage, in variance based methods one can work with arbitrary system as a black-box and calculations are based on inputs and outputs only. More recent works are concerned about expediting calculation pace [18, 58, 60]. The idea is to replace the system with an approximating function which gives benefits in sensitivity calculations, because it is easy to relate the output variances to the input variables.

We expand the variance of output solution into components. Assume that we break the system output into components:

$$\Gamma = \Gamma_0 + \sum_i \Gamma_i + \sum_{i < j} \Gamma_{ij} + \dots \quad (1.72)$$

A single index shows dependency to a specific input variable, whereas more than one index shows interaction of input variables. If we consider input vector Θ to be of n components θ_i for $i = 1, \dots, n$, then $\Gamma_i = f_i(\theta_i)$ and $\Gamma_{ij} = f_{ij}(\theta_i, \theta_j)$. In practice, we consider a finite number of terms in Equation (1.72). The first order sensitivity index, so called Sobol index, is defined as follows [66]:

$$S_i = \frac{V[E(\Gamma | \theta_i)]}{V(\Gamma)}, \quad (1.73)$$

where $E(\Gamma | \theta_i)$ is the conditional expectation of output Γ given θ_i and V is the variance operator. Since θ_i can be fixed at any value in its uncertainty interval, each of those values produce a distinct expectation $E(\Gamma | \theta_i)$. Equation 1.73 is a measure for variations of these expectations, which indicates the direct contribution of parameter θ_i in the output variance. For more than one index, a higher-order Sobol index can be defined as:

$$S_{ij} = \frac{V[E(\Gamma | \theta_i, \theta_j)] - V[E(\Gamma | \theta_i)] - V[E(\Gamma | \theta_j)]}{V(\Gamma)}. \quad (1.74)$$

Here, $V[E(\Gamma | \theta_i, \theta_j)]$ is the variance of output expectations after fixing θ_i and θ_j . This index represents significance of variation in output generated from uncertainty in input variables together, i.e., the interaction of uncertain parameters. If we add all indices that contain variable θ_i , the sum is called the total Sobol index:

$$S_{Ti} = S_i + \sum_{j \neq i} S_{ij} + \sum_{j \neq i} \sum_{k \neq i} S_{ijk} + \dots \quad (1.75)$$

To clarify the subject, we go through a simple analytical example given in [6]. Suppose that the exact expression for response Γ to be known and can be written as a polynomial with parameters θ_1 , θ_2 , and θ_3 :

$$\Gamma(\theta_1, \theta_2, \theta_3) = \theta_1^2 + \theta_2^4 + \theta_1\theta_2 + \theta_2\theta_3^4. \quad (1.76)$$

The Sobol indices can be calculated from functions F that are defined based on orthogonality condition used to decompose the solution and for input with Gaussian distribution Φ_n in uncertainty domain R^n they are as follows:

$$F_0 = \int_{R^n} \Gamma(\Theta) \Phi_n(\Theta) d\Theta, \quad (1.77)$$

$$F_i = \frac{\int_{R^{n-1}} \Gamma|_{\theta_i} \Phi_{n-1}(\theta_{\sim i}) d\theta_{\sim i}}{\Phi_1(\theta_i)} - F_0, \quad (1.78)$$

$$F_{i,j} = \frac{\int_{R^{n-2}} \Gamma|_{\theta_i, \theta_j} \Phi_{n-2}(\theta_{\sim i}, \theta_j) d\theta_{\sim i} d\theta_j}{\Phi_2(\theta_i, \theta_j)} - F_0 - F_i(\theta_i) - F_j(\theta_j). \quad (1.79)$$

$\Gamma|_{\theta_i}$ and $\Gamma|_{\theta_i, \theta_j}$ are the Γ values at fixed θ_i and $\{\theta_i, \theta_j\}$ respectively. $\theta_{\sim i}$ is the vector of dummy variables corresponding to all but the component θ_i of uncertain parameters Θ .

Let us denote the variances by D :

$$D = V[F(\Theta)] = \int F^2(\Theta) d\Theta - F_0, \quad (1.80)$$

that can be decomposed into

$$D_i = \int F_i^2(\theta_i) d\theta_i, \quad (1.81)$$

and

$$D_{i,j} = \int F_{i,j}^2(\theta_i, \theta_j) d\theta_i d\theta_j. \quad (1.82)$$

Then the Sobol indices can be found from:

$$S_i = \frac{D_i}{D}, \quad (1.83)$$

$$S_{i,j} = \frac{D_{i,j}}{D}. \quad (1.84)$$

Finally, the total Sobol index can be found from Equation 1.75. Applying the calculations of Equations 1.77 to 1.82 for our example (i.e., the expression in Equation 1.76) we can obtain the following Sobol indices, assuming Gaussian distributions for the parameters over the interval $[0, 1]$:

$$S_1 = 0.0005 \quad S_2 = 0.4281 \quad S_3 = 0.0000$$

$$S_{12} = 0.0007 \quad S_{13} = 0.0000 \quad S_{23} = 0.5708$$

$$S_{123} = 0.0000$$

and the total sobol indices are:

$$S_{T1} = 0.0012 \quad S_{T2} = 0.9996 \quad S_{T3} = 0.5708.$$

The total Sobol index can be used as a sensitivity measure to rank parameters for their influence in the results variation. In this example, we can see that the ranking that the total Sobol indices suggests is consistent with what can be inferred directly from the simple expression in Equation 1.76: θ_2 is the most influential parameters, because it appears in two terms, and in one of them with a forth degree. Interactions are represented by two indices, and S_{13} is zero, because there exist no term in Equation 1.76 that contains both θ_1 and θ_3 .

With known polynomial coefficients, Sobol indices are easy to calculate. When the number of parameters is large, it is possible to do initial sensitivity analysis with lower degree polynomials to filter out pertinent parameters. Then the analysis continues on the filtered parameters with a higher degree polynomial approximation.

1.10.4 Risk analysis

The risk is the impact of uncertainty on objectives. Quantifying the risk requires calculating this impact, which consist of two parts: quantification of the uncertainty and evaluation of the system consequences. Risk R of a process is quantitatively defined as the consequence C caused by the process multiplied by the probability P of that consequence to happen:

$$R = P \times C. \quad (1.85)$$

In the case of CO₂ injection into deep aquifers, the amount of CO₂ which stays mobile and undissolved in the medium for a time after injection can be considered as a consequence, bearing the potential of leakage up to the surface if exposed to a geological leakage point. The risk could be the expected amount of CO₂ that will leak through ill-plugged abandoned wells or cracks in the sealing rocks.

We consider looking at responses and the probability of them to happen. We initially examine this probability by drawing the histogram of response values obtained from detailed simulations on large number of realizations and corresponding to important time, like end of injection and end of simulation. Yet larger number of points in the uncertain parameter space are studied employing the data-driven aPC method, which requires a considerably short time for evaluating the responses. This way it is possible to perform an intensive Monte-Carlo process in a full tensor grid of input parameter variational space, resulting in a high resolution output probability distribution.

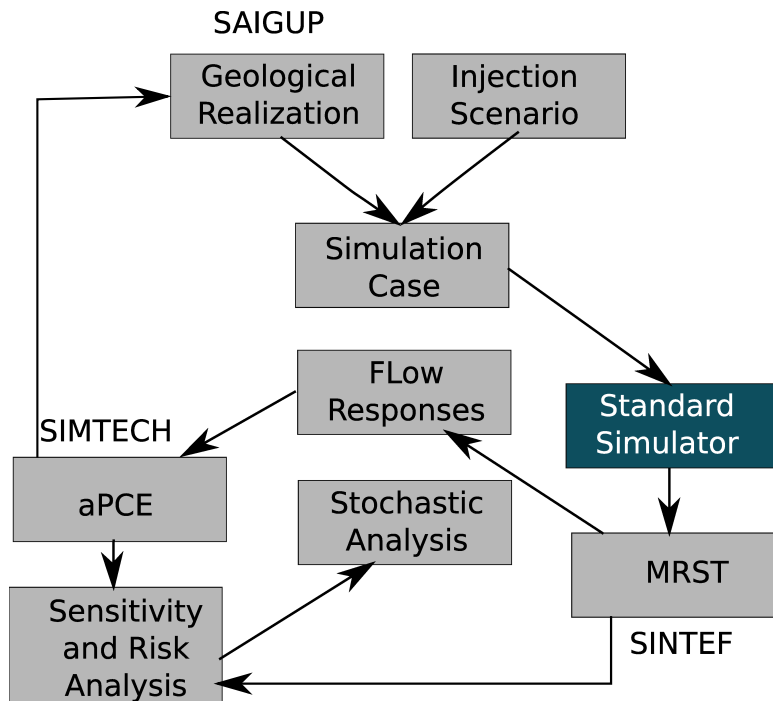


Figure 1.32: Flow-chart of work process implemented in an automated procedure.

1.11 Implementation of work-flow

This thesis incorporated working with large number of realizations, various flow scenarios, and different procedures and softwares. While the study progresses, new ideas and challenges rises that require manipulation of parts of the work-flow. In order to achieve the defined goals of the research, an automated work-flow is required that connects different parts of the study and converts data type in-between them. This makes the study feasible in terms of saving time for any necessary modifications.

Matlab programming language is used for implementing the work-flow in this research. The main reason for this choice, apart from the rich facilities available within Matlab toolboxes, is to use many functions within the Matlab Reservoir Simulation Toolbox (MRST) [44, 48] available as free and open-source software in Matlab language. For flow simulation a commercial software is used, which is a standard simulator for oil and gas industry and research. The simulator is using finite difference for flow modeling.

Figure 1.32 shows the elements of the work-flow implemented by a large number of Matlab functions. Functions from MRST at SINTEF and the stochastic tools of SIMTECH group in Stuttgart university are utilized and merged into the work-flow. The design is made such that the work-flow is flexible and general. Some research has been done by replacing the commercial simulator with in-house simulators at SINTEF, but the main study was performed using the black-box commercial simulator.

One thing to notice in Figure 1.32 is the link between designing geological realizations and implementation of aPCE method. A normal procedure must start by finding the collocation points from the given geological uncertainty, and then based on those collocation points we design the geological realizations.

Chapter 2

Introduction to the papers

2.1 Introduction

The main scientific part of this thesis consist of five papers. They come in a sequence to show the research progress withing this PhD program. Paper I is presented in the proceedings of the Computational Methods in Water Resources (CMWR) conference in Barcelona, 2010. Utilizing the feed back from that conference and including more uncertain parameters in the study ended up in paper II presented in the proceedings of the ECMOR XII in Oxford, 2010. Paper III includes a detailed study on the flow responses and effect of relative permeability on the flow and it is submitted to the International Journal of Greenhouse Gas Control (IJGGC). Pressure is an important model response during injection operations. Therefore, a special study is dedicated to pressure analysis in the system. This is reported in paper IV, which is submitted to the IJGGC. Finally, paper V reports modern stochastic techniques used to perform detailed quantitative sensitivity analysis and probabilistic risk assessments. This paper is submitted to special issue of the IJGGC.

2.2 Summary of papers

Paper I: Impact of geological heterogeneity on early-stage CO₂ plume migration

Summary:

It is a conventional practice in the context of CO₂ storage study to simplify the geological modeling in order to achieve an easier force balance study in the medium. Assuming a homogeneous medium is the first step to quantify the time and space scales in CO₂ storage problems by a dimensionless analysis on the analytical solution of flow equation. However, in practice the real flow performance is very much influenced by geological heterogeneity.

We use a set of SAIGUP realizations selected to cover the variability of four sedimentological and structural parameters. The selected parameters are lobosity, barriers, aggradation angle, progradation direction. Each of these parameters varies over three levels, except the progradation direction, which includes up-dip and down-dip directions. Combining the available parameters makes 54 realizations.

30 years of injection and 70 years of early migration of CO₂ are simulated and flow responses related to the storage capacity and leakage risk objectives are defined and calculated from the simulation results. The responses are reported in scatter plots at end of injection and end of early migration time.

This work is specific in examining how heterogeneity influences flow behavior by using a number of geological realizations. Flow responses defined in this work are specific to CO₂ studies and differ from the responses used in the original SAIGUP project to study oil recovery. We simulate the aquifer average pressure, model boundary fluxes, residual and mobile CO₂ saturation, and spatial distribution of connected CO₂ volumes. These responses can be considered to discuss the site storage capacity and risk of CO₂ leakage to surface.

Comments:

This work initially is presented in Edinburgh 2010 ACM conference, in a brief proceedings presentation, and more details of the work are reported in a proceedings for CMWR 2010 conference in Barcelona. The aim of this paper is to investigate the impact of geological heterogeneity on a typical CO₂ injection problem.

The main concern here is to include realistic geological heterogeneity knowledge into flow simulation work-flow, which is specific to the CO₂ storage problem. Results of this work conclude that the range of variability in flow responses indicate the significance of geological heterogeneity in modeling the CO₂ flow. Geological features are ranked by for their impact on each of the defined flow responses and in particular, aggradation angle has shown a big impact in most of the responses.

This paper received a comment on lacking the quantitative sensitivity analysis. This was added in the later works.

Paper II: *Impact of geological heterogeneity on early-stage CO₂ plume migration: sensitivity study*

Summary:

In this paper, we consider faults in addition to the four geological parameters used in Paper I. In the SAIGUP study, fault modeling is performed in an intensive variability over structural parameters and transmissibility across the fault. In order to keep the work less succinct and conclusive in studying the dynamics of flow, we fix the structural variability in its medium level and vary the transmissibility over three main levels: unfaulted, open faults and closed faults.

The flow responses analyzed are the same as defined in Paper I. In addition, we perform a linear sensitivity analysis for the flow responses with respect to the geological variations. The outcome of sensitivity analysis shows that the flow behavior is highly sensitive to aggradation angle. Barriers and faulting will also influence the flow responses significantly. In this work, similar to the previous report, we clearly see the range variation in flow responses that indicates how significant is to model the geological features accurately.

Comments:

The following issues have been addressed for the works reported in this paper:

- *The SAIGUP realizations*

This paper is presented in ECMOR conference in Oxford, 2010. This is a complementary to proceedings works presented in ACM Edinburgh, 2009 and CMWR in Barcelona, 2010.

Topography is a major player in the gravity dominated flow behavior. The SAIGUP realizations include variability in topography of the geological layering via structural changes due to faults and also barriers in the model. These are good enough for early migration when the CO₂ and water segregate and plumes accumulate below cap-rock and start the longer migration. In the long-term migration, top surface geometry is an important geological parameter and larger models than the SAIGUP models with a better resolution of the top surface are needed to get good predictions of the long-term migration phase. This was considered in the next generation of geological studies performed following this study [56, 67] under the IGEMS research project.

- *Physical assumptions*

The work concentrates on how geological heterogeneity impacts the flow performance. We need to measure the volumetric sweep efficiency of CO₂ plumes to evaluate the residual trapping. The most important parameter is the rock transmissibility, rather than fluid properties. Including more physics in the modeling will add the computational costs specially when the flow modeling is used in a sensitivity analysis or risk assessment process. Therefore, we used simple fluid models for PVT.

To accelerate the flow, we used linear relative permeability curves. This increases the flow mobility in the low saturation values. Hysteresis effects are modeled by changing the endpoints in the relative permeability curves and no scanning-curves is considered here. During injection, the main process is drainage. After injection, the imbibition process starts and mostly is a replacement of CO₂ by water due to gravity segregation. This justifies the usage of simple hysteresis model, and more detailed study can be done to investigate this influence in a quantitative manner.

- *Uncertainty considerations*

The geological parameters are changed in value between low and high levels. These values are assumed with the same probability, which is a reasonable start point for sensitivity analysis. In general, this probability might not be uniform, depending to the regional geology of the storage site.

Paper III: Impact of geological heterogeneity on early-stage CO₂ plume migration: sensitivity study

Summary:

In this paper, we use the same setup that is used in the previous paper. Five geological features are examined, which are lobosity, barriers, aggradational angle, progradational direction, and faults. Also, the same injection scenario is used: 30 years of CO₂ injection and 70 years of early migration. The injector is controlled by a constant rate and no pressure constraint is set to allow for all ranges of pressure, including those that are unrealistic. Moreover, we define an additional model output that is related to the risk of CO₂ leakage through any breakings in the cap-rock.

We examine the influence of simplifying assumptions considered in our works regarding linearity of relative permeability function. We perform a detailed flow analysis on various geological realizations using two different relative permeability relations: linear and quadratic functions. The non-linearity in relative permeability hinders the flow in the lower saturation values of the displaced phase, i.e., water phase. We discuss the influence of curvature on CO₂ flow dynamics within the aquifer.

Comments:

Results show that using linear relative permeability function ends up in conservative conclusions with respect to CO₂ distributions in the domain in terms of storage safety. Since computational costs are much lower for linear relative permeability scenario than quadratic relative permeability, it sounds a good strategy to perform sensitivity analysis by using linear relative permeability function on flow responses that are based on CO₂ distribution in the domain.

However, dramatic pressure build-up can happen in the medium during injection in the quadratic relative permeability scenario. This suggests that for pressure studies we must use more realistic relative permeability functions.

Following this work, a detailed pressure study with more realistic relative permeability curves is performed, which is reported in the next paper.

Paper IV: Geological storage of CO₂: heterogeneity impact on pressure behavior

Summary:

After observing the influence of relative permeability curvature on pressure response for CO₂ injection studies, in this paper we perform a detailed pressure study on the chosen geological realizations.

Pressure is an important criteria that can determine the success and failure of CO₂ storage operations. Over-pressurized injections can induce new fractures and open the existing faults and fractures that increases the risk of leakage for the mobile CO₂ in the domain. On the other hand, the pressure disturbance imposed on the system travels within the domain beyond the scales of CO₂ distribution. If the CO₂ is injected into a saline aquifer connected to fresh water aquifers, the pressure pulse may result in fresh water contaminations by the brine far from the injection point. We define specific pressure responses to examine the pressure disturbance in the system during injection.

Two injection scenarios are examined for the same 160 geological realizations setup. In the first scenario, the injector is set to a fixed volumetric rate to inject the CO₂ volume in 30 years into the domain, allowing for an unlimited pressure build-up. In the second scenario, a pressure constraint is set on the injector that results in various rates of injection in different geological realizations to inject the same amount of CO₂ volume considered in the first injection scenario.

Comments:

Pressure response sensitivity study with respect to different geological features indicates the significance of aggradational angle, progradational direction, and faults during injection. A probabilistic pressure analysis is also performed based on the 160 simulations on the available realizations.

Paper V: Geological storage of CO₂: global sensitivity analysis and risk assessment using the arbitrary polynomial chaos expansion**Summary:**

In this paper, we perform a stochastic sensitivity and risk analysis. We obtain a high resolution global sensitivity and probabilistic study on the flow responses that are defined and discussed in the previous papers. We choose barriers, aggradation angle, and faults from the SAIGUP geological parameters. Faults are considered by changing the transmissibility value across them, which is a continuous parameter. One more parameter is added to the study which is common in the literature and models the external pressure support from other aquifers attached to the model (regional groundwater effect).

Flow simulation on high resolution variational geology demands a huge computational costs. To enhance the calculation speed, we use a data-driven method that does not need to solve the full physical flow equations. We approximate the flow solver by a response surface method that is a polynomial and relates the system output to the input with a minimal computational cost. We use the arbitrary polynomial chaos expansion (aPC) to approximate the flow responses. The aPC method considers the uncertainty in the input variables.

A global sensitivity analysis is performed by employing Sobol indices that are based on variances of responses. The method is shown to be robust in problems of high levels of complexity and non-linearity.

And finally, we perform a Monte-Carlo process using the approximating polynomial on a high resolution input variations. This makes it possible to perform a high resolution probabilistic study on the flow responses. This way, extreme cases can be identified by probability of occurrence.

Comments:

In order to implement our stochastic technique, we choose geological parameters in this study that can be interpolated between two levels of their values. For example, it makes sense to use barriers coverage level of 25% between the low (10%) and medium (50%) levels used in the previous studies. Some of the geological parameters are discrete and can not be interpolated between two values. For instance, lobosity can only be varied over three points and we can not define a 1.5-lobe.

Having a large number of points in the input values interval requires intensive geological modelings to be used in the flow simulations. Using the data-driven polynomial, the approach only needs evaluating the polynomial in the defined values, and there is no need for full geological modeling except in the collocation points, i.e., point values that the polynomial coefficients must be calculated.

The work reported here is to demonstrate the work-flow of using the aPC for global sensitivity analysis and probabilistic risk assessment. A normal work-flow starts by defining the uncertainties in the input parameters and follows by building the geological models that are based on those uncertainties. To perform this study on the SAIGUP models that are consistent with a uniform uncertainty in the geological parameters, with no loss of generality, we used uniform uncertainty distributions for our study. However, the aPC method is not limited to uniform uncertainty descriptions.

Geological features are ranked based on the sensitivity analysis results. The results are in agreement with dynamics of the flow in the aquifer. Aggradation angle is the most influential parameter, while the regional groundwater has the least influence in the model responses. The study is not limited to the assumed uncertainty of input parameters and the conclusion may change for a very different uncertainty description.

Chapter 3

Scientific results

Paper I

3.1 Impact of geological heterogeneity on early-stage CO₂ plume migration: pressure behavior study

M. Ashraf, K.A. Lie, H.M. Nilsen & A. Skorstad

Submitted to *International Journal of Greenhouse Gas Control (IJGGC)*



EKSPRESS - OVER NATTEN

Sender	Melsdawn Ashrraf # 305, Sandgate 2 7012 Trondheim Norway
Mottakers navn	Matematisk institutt (UiB)
Reiser	Møll Sjøhder
Postkod	7800, 5020 BERGEN
Leveringsadresse (merk riktig postnummer for gate/vei)	
Postnummer	5020 Bergen, Norway
Telefonnr	

SM 23 441 998 0 NO

Kvittering (beholdes av sender)

Bring er heleid av Posten Norge AS. Vi hjelper bedriftene med alt innen logistikk - det vil si transportere, planlegge og lagra.

Denne delen er kvittering. Riv av og ta vare på den før du leverer pakken til Posten

- Kollinummeret er ditt referansenummer som du må bruke ved sporing av pakken. Ved å oppgi kollinummeret til mottaker, kan mottaker selv spore pakken.
- For sporing av pakke, levering på døren og informasjon om produkttilbuet
 - bring.no/barcodes
 - Kundeservice tlf 04045
- Her får du også informasjon om forsikringsvilkår, leveringsvilkår og farlig gods.

Paper II

3.2 Geological storage of CO₂: heterogeneity impact on pressure behavior

M. Ashraf

Submitted to *International Journal of Greenhouse Gas Control (IJGGC)*



EKSPRESS – OVER NATTEN

Sender	Melsønn Ashraf # 305, Sandgata 2 7012 Trondheim Norway
Mottakers navn	Matematisk institutt (UiB)
Reiser mål	Schoder
Postkrets	7800, 5020 BERGEN
Leveringsadresse (Merk rettig postnummer for gate/vei)	
Postnummer	5020 Bergen, Norway
Gate/vei (ikke bruk postbokAdresse)	
Telefonnr.	

Kvittering (beholdes av sender)

Bring er heleid av Posten Norge AS. Vi hjelper bedrifter med alt innen logistikk - det vil si transportere, planlegge og lagre.

Denne delen er kvittering. Riv av og ta vare på den før du leverer pakken til Posten

- Kollonummeret er ditt referansenummer som du må bruke ved sporing av pakken. Ved å oppgi kollonummeret til mottaker, kan mottaker selv spore pakken.
- For sporing av pakke, levering på døren og informasjon om produktibudet
 - bring.no/parcels
 - Kundeservice tlf 04045
- Her får du også informasjon om forsikringsvilkår, leveringsvilkår og farlig gods.

SM 23 441 998 0 NO

Paper III

3.3 Geological storage of CO₂: global sensitivity analysis and risk assessment using the arbitrary polynomial chaos expansion

M. Ashraf, S. Oladyshkin, W. Nowak

Submitted to the special issue of *International Journal of Greenhouse Gas Control (IJGGC)*



EKSPRESS – OVER NATTEN

Sender Meldam Ashraf # 305, Sandgata 2 7012 Trondheim Norway	Mottakers navn Matematisk institutt (UiB) Rever Mölli Schröder Post Books 7800, 5020 BERGEN	Levertid Gate/vei [Ikke bruk postbokadresse] Postnummer 5020 Bergen Norway Telefonnr.	SM 23 441 998 0 NO
---	--	---	--------------------

Kvittering (beholdes av sender)

Bring er heleid av Posten Norge AS. Vi hjelper bedrifter med alt innen logistikk - det vil si transportere, planlegge og lagre.

Denne delen er kvittering. Riv av og ta vare på den før du leverer pakken til Posten

- Kollonummeret er ditt referansenummer som du må bruke ved sporing av pakken. Ved å oppgi kollonummeret til mottaker, kan mottaker selv spore pakken.

- For sporing av pakke, levering på døren og informasjon om produktibudet
 - bring.no/parcels
 - Kundeservice tlf 04045

Her får du også informasjon om forsikringsvilkår, leveringsvilkår og farlig gods.

Bibliography

- [1] AAVATSMARK, I. Bevarelsesmetoder for elliptiske differensialligner. <http://www.mi.uib.no/~aavat/elliptisk.pdf>, 2004. 1.6.1
- [2] AAVATSMARK, I. Bevarelsesmetoder for hyperbolske differensialligner. <http://www.mi.uib.no/~aavat/hyperbolisk.pdf>, 2004. 1.6.1
- [3] ABRAMOWITZ, M., AND STEGUN, I., A. *Handbook of Mathematical Functions with Formulas, Graphs, and Mathematical Tables*. New York: Dover, 1965. 1.10.2
- [4] ALKAN, H., CINAR, Y., AND ÜLKER, E. Impact of capillary pressure, salinity and in situ conditions on co₂ injection into saline aquifers. *Transport in porous media* 84, 3 (2010), 799–819. 1.7.1
- [5] ALLEN, F., AND PUCKETT, D. Theoretical and experimental studies of rate-dependent two-phase immiscible flow. *SPE Production Engineering* 1, 1 (1986), 62–74. 1.7.1
- [6] ARWADE, S., MORADI, M., AND LOUGHJALAM, A. Variance decomposition and global sensitivity for structural systems. *Engineering Structures* 32, 1 (2010), 1–10. 1.10.3
- [7] BACHU, S. Sequestration of CO₂ in geological media: criteria and approach for site selection in response to climate change. *Energy Conversion and Management* 41, 9 (2000), 953–970. 1.1
- [8] BASHORE, W., ARAKTINGI, U., LEVY, M., AND SCHWELLER, W. The importance of the geological model for reservoir characterization using geostatistical techniques and the impact on subsequent fluid flow. In *SPE Annual Technical Conference and Exhibition* (1993). 1.1
- [9] BEAR, J. *Dynamics of fluids in porous media*. Dover publications, 1988. 1.6.1
- [10] BENSON LAB, S. U. Relative pereability explorer(rpe). <http://pangea.stanford.edu/research/bensonlab/relperm/index.html>. 1.6.2
- [11] BENTSEN, R. Effect of neglecting viscous coupling and dynamic capillary pressure on the one-dimensional flow of two immiscible phases through a porous medium. *SPE paper*, 026016 (1993). 1.7.1
- [12] BINNING, P., AND CELIA, M. Practical implementation of the fractional flow approach to multi-phase flow simulation. *Advances in water resources* 22, 5 (1999), 461–478. 1.6.2
- [13] BRADSHAW, J., AND COOK, P. Geological sequestration of carbon dioxide. *Environmental Geosciences* 8, 3 (2001), 149. 1.1
- [14] CAERS, J., AND ZHANG, T. Multiple-point geostatistics: a quantitative vehicle for integrating geologic analogs into multiple reservoir models. *AAPG* (2002). 1.5
- [15] CELIA, M., AND NORDBOTTEN, J. *Geological Storage of CO₂: Modeling Approaches for Large-Scale Simulation*. Wiley, 2011. 1.6.1, 1.1, 1.2, 1.8

- [16] CHEN, Z., BODVARSSON, G., AND WITHERSPOON, P. An integral equation formulation for two-phase flow and other nonlinear flow problems through porous media. In *SPE Annual Technical Conference and Exhibition* (1990). [1.7.1](#)
- [17] CLASS, H., EBIGBO, A., HELMIG, R., DAHLE, H., NORDBOTTEN, J., CELIA, M., AUDIGANE, P., DARCIS, M., ENNIS-KING, J., FAN, Y., ET AL. A benchmark study on problems related to CO₂ storage in geologic formations. *Computational Geosciences* 13, 4 (2009), 409–434. [1.8](#)
- [18] CRESTAUX, T., ET AL. Polynomial chaos expansion for sensitivity analysis. *Reliability Engineering & System Safety* 94, 7 (2009), 1161–1172. [1.10.3](#)
- [19] DONG, M., AND DULLIEN, F. Effect of capillary forces on immiscible displacement in porous media. In *SPE Annual Technical Conference and Exhibition* (1999). [1.7.1](#)
- [20] DUAN, Z., AND ZHANG, Z. Equation of state of the h₂o, co₂, and h₂o-co₂ systems up to 10 gpa and 2573.15 k: Molecular dynamics simulations with ab initio potential surface. *Geochimica et cosmochimica acta* 70, 9 (2006), 2311–2324. [1.6.2](#)
- [21] EATON, T. On the importance of geological heterogeneity for flow simulation. *Sedimentary Geology* 184, 3-4 (2006), 187–201. [1.1](#), [1.5](#)
- [22] ELENIUS, M., AND JOHANNSEN, K. On the time scales of nonlinear instability in miscible displacement porous media flow. *Computational Geosciences* (2012), 1–11. [1.7.2](#)
- [23] ELENIUS, M., NORDBOTTEN, J., AND KALISCH, H. Effects of a capillary transition zone on the stability of a diffusive boundary layer. [1.7.2](#)
- [24] ELENIUS, M., TCHELEPI, H., AND JOHANNSEN, K. CO₂ trapping in sloping aquifers: High resolution numerical simulations. In *XVIII International Conference on Water Resources, CIMNE, Barcelona* (2010). [1.7.2](#)
- [25] FAJRAOUI, N., RAMASOMANANA, F., YOUNES, A., MARA, T. A. AND ACKERER, P., AND GUADAGNINI, A. Use of global sensitivity analysis and polynomial chaos expansion for interpretation of non-reactive transport experiments in laboratory-scale porous media. *Water Resour. Res.*, doi:10.1029/2010WR009639 (2011). [1.10.2](#)
- [26] FARAJZADEH, R., AND BRUINING, J. An analytical method for predicting the performance of gravitationally-unstable flow in heterogeneous media. In *SPE EUROPEC/EAGE Annual Conference and Exhibition* (2011). [1.7.1](#)
- [27] FAYERS, F., AND SHELDON, J. The effect of capillary pressure and gravity on two-phase fluid flow in a porous medium. *Trans. AIME* 216 (1959), 147. [1.7.1](#)
- [28] FLETT, M., GURTON, R., AND WEIR, G. Heterogeneous saline formations for carbon dioxide disposal: Impact of varying heterogeneity on containment and trapping. *Journal of Petroleum Science and Engineering* 57, 1-2 (2007), 106–118. [1.5.1](#)
- [29] FOO, J., AND KARNIADAKIS, G. Multi-element probabilistic collocation method in high dimensions. *Journal of Computational Physics* 229, 5 (2010), 1536–1557. [1.10.2](#)
- [30] FOUKAL, P., FRÖHLICH, C., SPRUIT, H., AND WIGLEY, T. Variations in solar luminosity and their effect on the earth's climate. *Nature* 443, 7108 (2006), 161–166. [1.2](#)
- [31] GHANEM, R., AND SPANOS, P. A stochastic galerkin expansion for nonlinear random vibration analysis. *Probabilistic Engineering Mechanics* 8 (1993), 255–264. [1.10.2](#)

- [32] GRAY, W., HERRERA, P., GASDA, S., AND DAHLE, H. Derivation of vertical equilibrium models for CO₂ migration from pore scale equations. *International Journal of Numerical Analysis and Modeling* (2011). [1.8](#)
- [33] GREENWOOD, H. The compressibility of gaseous mixtures of carbon dioxide and water between 0 and 500 bars pressure and 450 and 800 centigrade. *Am. J. Sci.* 267 (1969), 191–208. [1.6.2](#)
- [34] GUNTER, W., WIWEHAR, B., AND PERKINS, E. Aquifer disposal of co 2-rich greenhouse gases: extension of the time scale of experiment for co 2-sequestering reactions by geochemical modelling. *Mineralogy and Petrology* 59, 1 (1997), 121–140. [1.2](#), [1.7.2](#)
- [35] HADLEY, G., AND HANDY, L. A theoretical and experimental study of the steady state capillary end effect. In *Fall Meeting of the Petroleum Branch of AIME* (1956). [1.7.1](#)
- [36] HASSANZADEH, H., POOLADI-DARVISH, M., AND KEITH, D. Modelling of convective mixing in co storage. *Journal of Canadian Petroleum Technology* 44, 10 (2005). [1.7.2](#)
- [37] HITCHON, B., GUNTER, W., GENTZIS, T., AND BAILEY, R. Sedimentary basins and greenhouse gases: a serendipitous association. *Energy Conversion and Management* 40, 8 (1999), 825–843. [1.1](#)
- [38] HOUGHTON, J., ET AL. *Climate change 2001: the scientific basis*, vol. 881. Cambridge University Press Cambridge, 2001. [1.1](#)
- [39] HOWELL, J., SKORSTAD, A., MACDONALD, A., FORDHAM, A., FLINT, S., FJELLVOLL, B., AND MANZOCCHI, T. Sedimentological parameterization of shallow-marine reservoirs. *Petroleum Geoscience* 14, 1 (2008), 17–34. [1.5.2](#)
- [40] ISUKAPALLI, S., S., ROY, A., AND GEORGOPoulos, P., G. Stochastic response surface methods (srsm) for uncertainty propagation: Application to environmental and biological systems. *Risk Analysis* 18, 3 (1998), 351–363. [1.10.2](#)
- [41] JANG, Y., S., SITAR, N., AND KIUREGHIAN, A., D. Reliability analysis of contaminant transport in saturated porous media. *Water Resources Research* 30, 8 (1994), 2435–2448. [1.10.3](#)
- [42] KEESE, A., AND MATTHIES, H. G. Sparse quadrature as an alternative to mc for stochastic finite element techniques. *Proc. Appl. Math. Mech.* 3 (2003), 493–494. [1.10.2](#)
- [43] LI, H., AND ZHANG, D. Probabilistic collocation method for flow in porous media: Comparisons with other stochastic methods. *Water Resources Research* 43 (2007), 44–48. [1.10.2](#)
- [44] LIE, K., KROGSTAD, S., LIGAARDEN, I., NATVIG, J., NILSEN, H., AND SKAFLESTAD, B. Open-source matlab implementation of consistent discretisations on complex grids. *Computational Geosciences* (2011), 1–26. [1.11](#)
- [45] LIE, K., LIGAARDEN, I., AND NILSEN, H. Accurate discretization of vertically-averaged models of CO₂ plume migration. *ECMOR XII–12th European Conference on the Mathematics of Oil Recovery, EAGE, Oxford, UK* (2010). [1.8](#)
- [46] LIGAARDEN, I., AND NILSEN, H. Numerical aspects of using vertical equilibrium models for simulating CO₂ sequestration. In *Proceedings of ECMOR XII–12th European Conference on the Mathematics of Oil Recovery, EAGE, Oxford, UK* (2010). [1.8](#)
- [47] MANZOCCHI, T., CARTER, J., SKORSTAD, A., FJELLVOLL, B., STEPHEN, K., HOWELL, J., MATTHEWS, J., WALSH, J., NEPVEU, M., BOS, C., ET AL. Sensitivity of the impact of geological uncertainty on production from faulted and unfaulted shallow-marine oil reservoirs: objectives and methods. *Petroleum Geoscience* 14, 1 (2008), 3–11. [1.5.2](#)

- [48] MATEMATHICS, S. A. Matlab reservoir simulation toolbox. <http://www.sintef.no/MRST>. 1.11
- [49] MATTHEWS, J., CARTER, J., STEPHEN, K., ZIMMERMAN, R., SKORSTAD, A., MANZOCCHI, T., AND HOWELL, J. Assessing the effect of geological uncertainty on recovery estimates in shallow-marine reservoirs: the application of reservoir engineering to the SAIGUP project. *Petroleum Geoscience* 14, 1 (2008), 35–44. 1.5.2
- [50] MATTHIES, H., AND KEESE., A. Galerkin methods for linear and nonlinear elliptic stochastic partial differential equations. *Comp. Meth. Appl. Mech. Engrg.* 194 (2005), 1295–1331. 1.10.2
- [51] MELICK, J., GARDNER, M., AND ULAND, M. Incorporating geologic heterogeneity in 3d basin-scale models for CO₂ sequestration: Examples from the powder river basin, ne wyoming and se montana. In *SPE International Conference on CO₂ Capture, Storage, and Utilization* (2009). 1.1
- [52] MILLIKEN, W., LEVY, M., STREBELLE, S., AND ZHANG, Y. The effect of geologic parameters and uncertainties on subsurface flow: deepwater depositional systems. In *SPE Western Regional and Pacific Section AAPG Joint Meeting* (2008). 1.1
- [53] MØLL NILSEN, H., HERRERA, P., ASHRAF, M., LIGAARDEN, I., IDING, M., HERMANRUD, C., LIE, K., NORDBOTTEN, J., DAHLE, H., AND KEILEGAVLEN, E. Field-case simulation of CO₂ plume migration using vertical-equilibrium models. *Energy Procedia* 4 (2011), 3801–3808. 1.8, 1.8
- [54] MORRIS, M., D. Morris factorial sampling plans for preliminary computational experiments. *Technometrics*, 33 (1991), 161–174. 1.10.3
- [55] MUSKAT, M. *The Flow of Homogeneous Fluids Through Porous Media*. Mac Graw Hill, New York, 1937. 1.6.1
- [56] NILSEN, H., SYVERSVEEN, A., LIE, K., TVERANGER, J., AND NORDBOTTEN, J. Impact of top-surface morphology on co₂ storage capacity. *International Journal of Greenhouse Gas Control* 11 (2012), 221–235. 2.2
- [57] NORDBOTTEN, J., CELIA, M., AND BACHU, S. Injection and storage of co 2 in deep saline aquifers: Analytical solution for co 2 plume evolution during injection. *Transport in Porous Media* 58, 3 (2005), 339–360. 1.7.1
- [58] OLADYSHKIN, S., CLASS, H., HELMIG, R., AND NOWAK, W. A concept for data-driven uncertainty quantification and its application to carbon dioxide storage in geological formations. *Advances in Water Resources* 34 (2011), 1508–1518, doi: 10.1016/j.advwatres.2011.08.005. 1.10.2, 1.10.2, 1.10.3
- [59] OLADYSHKIN, S., CLASS, H., HELMIG, R., AND NOWAK, W. An integrative approach to robust design and probabilistic risk assessment for CO₂ storage in geological formations. *Computational Geosciences* 15, 3 (2011), 565–577, doi: 10.1007/s10596-011-9224-8. 1.10.2, 1.10.2
- [60] OLADYSHKIN, S., DE BARROS, F. P. J., AND NOWAK, W. Global sensitivity analysis: a flexible and efficient framework with an example from stochastic hydrogeology. *Advances in Water Resources In Press* (2011), doi: 10.1016/j.advwatres.2011.11.001. 1.10.3
- [61] RAPOPORT, L., AND LEAS, W. Properties of linear waterfloods. *Trans. AIME* 198, 1953 (1953), 139–148. 1.7.1
- [62] REUTER, U., AND LIEBSCHER, M. Global sensitivity analysis in view of nonlinear structural behavior. In *Proceedings of the 7th LS-Dyna Forum, Bamberg* (2008). 1.10.1, 1.10.3

- [63] ROSADO-VAZQUEZ, F., RANGEL-GERMAN, E., AND RODRIGUEZ-DE LA GARZA, F. Analysis of capillary, gravity and viscous forces effects in oil/water displacement. In *International Oil Conference and Exhibition in Mexico* (2007). [1.7.1](#)
- [64] SAHIMI, M. *Flow and transport in porous media and fractured rock: From classical methods to modern approaches*. Wiley-VCH, 2011. [1.6.1](#)
- [65] SALTELLI, A. Global sensitivity analysis: an introduction. In *Proc. 4th International Conference on Sensitivity Analysis of Model Output*, pp. 27–43. [1.10.1](#)
- [66] SALTELLI, A. *Global sensitivity analysis: the primer*. Wiley, 2007. [1.10.3](#), [1.10.3](#)
- [67] SYVERSVEEN, A., NILSEN, H., LIE, K., TVERANGER, J., AND ABRAHAMSEN, P. A study on how top-surface morphology influences the storage capacity of co₂ in saline aquifers. *Geostatistics Oslo 2012* (2012), 481–492. [1.8](#), [1.9.2](#), [2.2](#)
- [68] VAN DER MEER, L. The co₂ storage efficiency of aquifers. *Energy Conversion and Management* 36, 6 (1995), 513–518. [1.5.1](#)
- [69] VILLADSEN, J., AND MICHELSEN, M. L. *Solution of differential equation models by polynomial approximation*. Prentice-Hall, 1978. [1.10.2](#)
- [70] XIU, D., AND KARNIADAKIS, G. E. Modeling uncertainty in flow simulations via generalized polynomial chaos. *Journal of Computational Physics* 187 (2003), 137–167. [1.10.2](#)
- [71] YANG, W. An analytical solution to two-phase flow in porous media and its application to water coning. *SPE Reservoir Eng. J.*, 1 38 (1992). [1.7.1](#)
- [72] YORTSOS, Y., AND FOKAS, A. An analytical solution for linear waterflood including the effects of capillary pressure. *Old SPE Journal* 23, 1 (1983), 115–124. [1.7.1](#), [1.7.1](#)
- [73] ZHANG, D., AND LU, Z. An efficient, high-order perturbation approach for flow in random media via karhunen-loeve and polynomial expansions. *Journal of Computational Physics* 194 (2004), 773–794. [1.10.2](#)